https://doi.org/10.5194/egusphere-2023-1710
Preprint. Discussion started: 13 September 2023

Temporal and spatial variations in dust activity in Australia based on remote sensing and reanalysis data sets

Yahui Che[1], Bofu Yu[1], Katherine Bracco[1]

[1]School of Engineering and Built Environment, Griffith University, Brisbane, 4111, Australia

Correspondence to: Bofu Yu (b.yu@griffith.edu.au)

Abstract. Spatial and temporal variations in the level of dust activity can provide valuable information for policy making and climate research. Recently, MODIS aerosol products have been successfully used for retrieving dust aerosol optical depth (DAOD), especially over bright dust source areas and MERRA-2 aerosol reanalysis provides DAOD, and additionally other dust aerosol-related parameters. In this study, spatial and temporal variations in dust activity in Australia were analyzed using MODIS and MERRA-2 combined (M&M) DAOD and MERRA-2 near-surface dust concentrations/estimated PM10 for the period from 1980-2020. Validation results show that M&M DAOD has an expected error of $\pm(0.016 + 0.15\tau)$ compared to the ground observations at the AERONET sites. MERRA-2 near-surface dust concentrations show a power law relationship with visibility data collected at meteorological stations with an r^2 value from 0.18 to 0.44, and the estimated MERRA-2 PM10 shows similar temporal variations and correlates with ground-based PM10 data with an r^2 value from 0.14 to 0.44 at six selected stations in Australia. Moreover, MERRA-2 dust flux shows the same major dust pathways as those in previous studies and similar dust emissions/deposition areas. Dust events based on DAOD over eastern Australia are concentrated in the north in December, in the south in February, and can occur anywhere in January. Near-surface dust concentration was found to be the highest (over 200μg/m^3) over the center of Lake Eyre Basin in central Australia and radially decreased to the coast to below 20μg/m^3 via the two main pathways in the southwest and northeast. The ratio of near-surface dust concentration to PM10 shows a similar spatial pattern. Total dust emission was estimated to be 40 MT (mega-tonnes) per year over the period 1980-2020, of which nearly 50% was deposited on land and the rest exported away from the Australian continent.

1. Introduction

Dust storms as one natural disaster occur frequently in Australia, especially in the central inland area as the largest dust source in the Southern Hemisphere (Shao, 2009; McTainsh et al., 2011b; Ekström et al., 2004; McTainsh et al., 2011a), contributing to approximately 5% of the global total dust emissions (Shao, 2009; Wu et al., 2020;

https://doi.org/10.5194/egusphere-2023-1710
Preprint. Discussion started: 13 September 2023

Chen et al., 2022). Dust sourced from the Lake Eyre Basin is not only deposited on the Australian continent but also transported to the Tasman Sea in the southeast and the Indian Ocean in the northwest (Strong et al., 2011; Bowler, 1976; Sprigg, 1982; Speer, 2013; Ekström et al., 2004; Shao et al., 2007). The adverse impacts of dust storms on populated areas include incalculable economic loss in agriculture (Stefanski and Sivakumar, 2009) and household cleaning and associated activities (Tozer and Leys, 2013), human health issues such as respiratory problems (Roberts, 2013; Chen et al., 2007; Cowie et al., 2010; Goudie, 2014; Middleton, 2017) and cardiovascular disease (Domínguez-Rodríguez et al., 2021; Zhang et al., 2016), and contamination of water sources (Middleton, 2017). Moreover, the Australian dust over the south-west Pacific Ocean strengthens the relationship between rainfall and the El Niño Southern Oscillation (ENSO) by driving ENSO-related anomalies in radiative forcing (Rotstayn et al., 2011), which is the direct dust feedback to climate (Shao et al., 2013).

The severity of dust activities can be indicated by visibility-based dust event days/dust storm index (DSI) (Yu et al., 1992, 1993; McTainsh et al., 2011b; O'Loingsigh et al., 2017) and dust concentration (Shao et al., 2013; McTainsh et al., 2005; Tews, 1996; Baddock et al., 2014), aerosol optical depth (AOD)/DAOD (dust AOD) (Ginoux et al., 2010; Pu and Ginoux, 2018; Yu and Ginoux, 2021; Ginoux et al., 2012; She et al., 2018) and dust index (Di et al., 2016; Yang et al., 2023; Bullard et al., 2008), simulated near-surface dust concentration (Prospero et al., 2020; Buchard et al., 2017), and PM10 (particles with a diameter of 10 micrometers or less) (Leys et al., 2011; de Jesus et al., 2020). The dust event database (DEDB)/dust storm index (DSI) is widely used in dust and wind erosion research in Australia, especially for spatial and temporal variations in dust activities and has benefited from long-term temporal data and widely distributed Bureau of Meteorology (BoM) sites (McTainsh and Pitblado, 1987; McTainsh et al., 2011a; O'Loingsigh et al., 2014). Horizontal visibility has also been used for estimating dust concentration and dust loading for large dust storms (McTainsh et al., 2005) and visibility-based dust concentration has been even used for exploring the climate forcing of dust at the global scale (Shao et al., 2013). With development of satellite remote sensing and numerical dust models, remote sensing and General Circulation Model (GCM) products have been increasingly applied to dust research on spatial extent detection, columnar optical properties, and near-surface concentrations. Dust index based on satellite images can be traced back to the detection of dust storms using Advanced Very High-Resolution Radiometer (AVHRR) data (Ackerman, 1989), taking advantage of AVHRR's large spatial coverage. So far, several different dust indexes have been developed for regional or global dust detection and different sensors (Yang et al., 2023). Satellite data retrieved

https://doi.org/10.5194/egusphere-2023-1710
Preprint. Discussion started: 13 September 2023

AOD/DAOD have been more frequently applied to quantitative dust research since AOD was successfully retrieved over bright dust source areas (Hsu et al., 2004; Ginoux et al., 2010; Baddock et al., 2009). Benefiting from satellite providing dust source schemes (Ginoux et al., 2001), and near-surface dust concentration has been simulated for regions or at the global scale (Gelaro et al., 2017; Buchard et al., 2017; Shao et al., 2007; Wu et al., 2020).

Analysis of long-term AOD/DAOD data has not been attempted for Australia. AOD/DAOD was mostly used for identifying the spatial extent of single dust events or as reference data for evaluating dust detection algorithms in Australia. For example, Baddock et al. (2009) assessed the performances of four detection algorithms based on Moderate Resolution Imaging Spectroradiometer (MODIS) L1 (Level 1) B data and MODIS Deepblue (DB) AOD for central Australia (i.e. the Lake Eyre Basin) on identifying airborne dust and mineral aerosols. There are a few dust studies on analyzing seasonal spatial variations of dust using a multi-year AOD/DAOD dataset. Ginoux et al. (2012) retrieved global DAOD using MODIS DB aerosol dataset from 2003 to 2009 and analyzed major anthropogenic and natural dust emissions in Australia. Their results show that the contribution to total emissions by anthropogenic activities can be as high as 75% in Australia. Yu and Ginoux (2021) show the monthly MODIS DB DAOD and Multi-angle Imaging SpectroRadiometer (MISR) coarse mode AOD at 15 AERONET sites and the annual DAOD and coarse mode AOD in Australia from 2000 to 2019. The comparison with DSI shows that satellite AOD/DAOD presents the same dusty month/season as that by DSI at three AERONET sites in the dust source area. Yang et al. (2021) show similar AERONET coarse mode AOD variations and seasonal contribution of dust to total aerosols at nine AERONET sites and analyze seasonal DAOD from MERRA-2 aerosol reanalysis from the early 2000s to 2020. There are limitations to this kind of study. Firstly, MODIS DB retrieved DAOD shows much smaller coverage than the original DB AOD due to excluding low background DAOD, possibly resulting in overestimation of dust activity severity. Secondly, MERRA is very likely to have underestimated DAOD over 0.2, especially for severe dust storms such as those on the 23rd of October 2002 and 23rd of September 2009 (Che et al., 2022).

PM10 is often taken as an effective indicator of dust severity for single dust storms (Leys et al., 2011; McGowan and Clark, 2008); however, long-term analysis of dust severity for Australia is of great difficulty using PM10 data. First, PM10 observations in each state mostly began after 2000 in populated urban areas while the dust source

https://doi.org/10.5194/egusphere-2023-1710
Preprint. Discussion started: 13 September 2023

area in central Australia lacks PM10 observations. This spatial distribution of PM10 sites also causes difficulties in retrieving PM10 in Australia using satellite AOD. Second, little progress has been made to retrieve PM10 for large regions based on remote sensing products in Australia because 1) a reliable estimate of PM10 is difficult to obtain due to the relatively low dust concentrations approaching its retrieval uncertainty and 2) inclusion of AOD and related predictors cannot improve the accuracy of simulated PM10 (Pereira et al., 2017). Therefore, long-term time series analysis of PM10 in Australia has predominantly focused on site-based observations. For example, de Jesus et al. (2020) analyzed PM10 trends in major cities of Australia over the last two decades using site PM10 observations. Compared with PM10, near-surface dust concentration is capable of indicating the severity of dust events without providing information on the proportion of fine particles because PM10 observations include not only dust particles but also other types of particles. For example, Love et al. (2019) analyzed a 17-year (1990-2007) near-surface dust concentration data collected by a high-volume air sampler (HVS) in Mildura. Long-term dust analysis studies such as this are relatively few compared to those based on visibility-transferred dust concentrations. However, the accuracy of visibility-transferred dust concentration cannot be ensured. As noted by McTainsh et al. (2005), the relationships between visibility and dust concentration obtained in the United States of America (USA) (Chepil and Woodruff, 1957) and Australia in the 1990s (Tews, 1996) have been inappropriate for estimating dust concentration over different areas of Australia, since visibility-based dust concentrations are strongly influenced by dust particle size,.

Development of numerical dust models and GCMs provides dust cycle simulations for understanding the impacts of dust on the earth systems. Models such as the Georgia Tech/Goddard Global Ozone Chemistry Aerosol Radiation and Transport (GOCART) (Ginoux et al., 2001), Mineral Dust Entrainment and Deposition (DEAD) (Zender, 2003), and Aerosol Species IN the Global AtmospheRe (MASINGAR) coupled with MRI/JMA 98 GCM (Tanaka and Chiba, 2006) are all capable of providing dust cycles for regions around the world. However, dust emissions and depositions vary substantially among models (Chen et al., 2022; Wu et al., 2020). This would directly lead to a large discrepancy in conclusions based on different models. For example, the contribution of Australian dust to global dust emissions is estimated to vary from 0.02% to 27.8% using simulation outputs from 15 CMIP5 (Coupled Model Intercomparison Project Phase 5) models (Wu et al., 2020). Therefore, long-term analysis of the dust cycle in Australia needs a dataset with high accuracy and capability to quantify long-term trends and variabilities.

https://doi.org/10.5194/egusphere-2023-1710
Preprint. Discussion started: 13 September 2023

MODIS DB and MERRA-2 data products, dust aerosols, and near-surface dust concentration/PM10 observations were analyzed in this study for a better understanding of long-term dust entrainment and transport over Australia. Objectives of this study include:

1. To develop a DAOD dataset using MERRA-2 aerosol reanalysis and MODIS DB aerosol datasets;
2. Validate MERRA-2 near-surface dust concentrations using ground-based visibility data sets, and MERRA-2 estimated PM10 with ground-based PM10 observations sourced from the New South Wales Air Quality Monitoring Network (NSW AQMN);
3. To corroborate MERRA-2 dust flux with major dust pathways identified in previous studies;
4. To map the seasonal MODIS and MERRA-2 (M&M) DAOD from 2002 to 2020 and seasonal MERRA-2 near-surface dust concentrations/PM10 over the period from 1980 to 2020;
5. To quantify the annual dust cycle for Australia over the period from 1980 to 2020, including dust emission in Australia using MERRA-2 emission data, dust import and export using MERRA-2 flux data, and dust deposition using MERRA-2 emission and flux data.

2. Data and methodology

2.1 Ground-based PM10 and AERONET data

AOD at 440nm and Ångström exponent (AE) at 440-675nm from AERONET v3 solar products were used for calculating AOD at 550nm, as well as Level 1.5 (L1.5) single scattering albedo (SSA) at 440nm from v3 inversion product to retrieve DAOD. The latest AERONET v3 solar product includes data at Level 1.0 (L1.0) (without data screening), L1.5 (with cloud screened and quality controlled), and Level 2.0 (L2.0) (quality assured) (https://aeronet.gsfc.nasa.gov/). Giles et al. (2019) reported that AOD from the AEROENT V3 product was with a low uncertainty, suggested by a bias of +0.02 and one sigma uncertainty of 0.02. Since satellite AOD normally refers to that at 550nm, AE is necessarily used for spectrally interpolating AOD to this wavelength according to the dependence of AOD on wavelength (Angstrom, 1924). The Version 3 (V3) inversion product also includes data at three levels, L1.0, L1.5, and L2.0. The main difference between L1.5 and L2.0 is that the L2.0 inversion product is only made when the corresponding AOD is higher than 0.4 (Dubovik and King, 2000). This leads to the data volume of L2.0 SSA being far smaller than that of L1.5, especially over Australia predominated by low AOD conditions. L1.5 SSA data with a much larger data volume, therefore, was used for identifying dust-

https://doi.org/10.5194/egusphere-2023-1710
Preprint. Discussion started: 13 September 2023

143 contaminated AOD. In this study, all L2.0 AOD and AE, L1.5 SSA, as well as fine mode fraction (FMF) in the
144 Spectral Deconvolution Algorithm (SDA) database in Australia from 1997 to 2020 were used for retrieving DAOD
145 at 550nm (yellow stars in Fig.1).
146

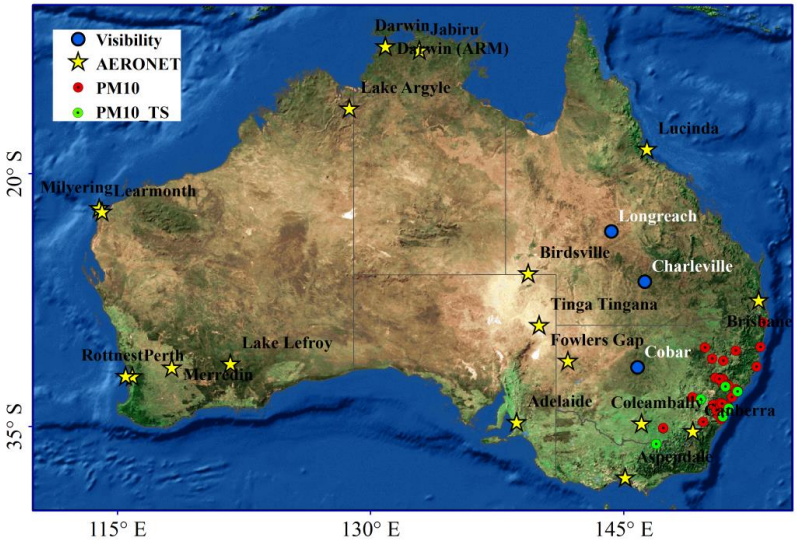

147

148 **Figure 1**: **Distribution of ground-based sites. Yellow stars are inland AERONET sites in Australia; Green**
149 **and red circles indicate PM10 observation sites for validating MERRA-2 products, among them time series**
150 **analysis was conducted at green sites; Circles in blue are visibility observation sites.**
151

152 Horizontal visibility records from the BoM were manually estimated and noted by a weather observer. All
153 visibility records have an upper limit of 10km, which means that if the record shows a visibility of 10km the actual
154 visibility could be 10km or greater. In addition to visibility, a synoptic code was recorded during notable weather
155 events such as dust storms (Baddock et al., 2014) as well as a weather type for the weather observation
156 immediately prior to the current observation (O'Loingsigh et al., 2010). There are 11 SYNOP (surface synoptic
157 observations) codes for dust weather, including dust haze, raised dust or sand, dust whirls, thunderstorm with sand
158 or dust storms, dust storms, and so on. Due to the visibility record only allocated one SYNOP code, the highest-
159 coded weather code was retained although it may have included several weather types (O'Loingsigh et al., 2010).
160 The long-term visibility records with SYNOP codes have been widely used for wind erosion research (McTainsh
161 et al., 1989b, 1990, 2011a), dust event climatologies including the DEDB and DSI developed at Griffith University

https://doi.org/10.5194/egusphere-2023-1710
Preprint. Discussion started: 13 September 2023

(McTainsh et al., 2011b; O'Loingsigh et al., 2014, 2010) and single dust events (Shao et al., 2007; McTainsh et al., 2005; Leys et al., 2011). In this study, all hourly BoM horizontal visibility data with a dust type SYNOP code (excluding thunderstorms) were used for validating MERRA-2 near-surface dust mass concentration at three sites (Charleville, Cobar, and Longreach, Fig.1) from 1980 to 2020.

PM10 concentrations are publicly downloadable from the NSW AQMN website (https://www.dpie.nsw.gov.au/). AQMN equips a Tapered Element Oscillating Element instrument (TEOM), measuring atmospheric particles < 10μm. The filter in the TEOM weighs collected samples every 2 seconds and the average value is reported hourly. Data quality control is applied to all PM10 databases according to Australian Standard 3580.9.8 (Leys et al., 2011). All PM10, gases, and climate observations data can be accessed using the AQMN web data download facility (https://www.dpie.nsw.gov.au/air-quality/air-quality-data-services/data-download-facility). In this study, monthly PM data from 62 AQMN urban sites (circles in green and red in Fig.1) were used for validating MERRA-2 near-surface dust concentrations from 2001 to 2020.

2.2 MERRA-2 aerosol reanalysis

MERRA-2 aerosol reanalysis provides long-term global aerosol parameter datasets from 1980 to the present (Randles et al., 2017; Gelaro et al., 2017; Buchard et al., 2017). MERRA-2 includes optical depth, near-surface mass concentrations, column mass concentrations, two directional mass flux for each aerosol component, including sea salt, sulfate in (SO4 and SO2), organic carbon, dust, and black carbon. Due to the inclusion of the GEOS and GSI assimilation system, MERRA-2 aerosol simulations perform comparably with high-quality satellite-based datasets and are fairly close to aerosol observations. Benefiting from the incorporation of space-based and ground-based observations, the accuracy for the total AOD is guaranteed with physical models outputs constrained by the assimilation system (https://gmao.gsfc.nasa.gov/research/science_snapshots/2015/MERRA2_global_aerosol_dist.php). In this study, MERRA-2 dust (DAOD) and total AOD were used for providing the ratio of dust aerosols over total particulate, all near-surface aerosol mass concentrations for estimating PM10, as well as, dust flux for estimating dust loading import/export for Australia.

Numerous validation studies have shown that MERRA-2 optical depth and near-surface concentrations could be used for temporal and spatial analysis and even long-term analysis of aerosols regionally or globally due to the

https://doi.org/10.5194/egusphere-2023-1710
Preprint. Discussion started: 13 September 2023

high quality and long temporal coverage from 1980 to the present. This kind of study primarily focuses on the validation of MERRA-2 AOD with ground-based AOD from AERONET (Buchard et al., 2017; Sun et al., 2019a; Che et al., 2022; Randles et al., 2017), SONET (Sun-Sky Radiometer Observation Network) (Ou et al., 2022), SKYNET (Sun et al., 2019b). For dust research in Australia, MERRA-2 AOD has been validated/evaluated with AERONET (Che et al., 2022; Mukkavilli et al., 2019) and MODIS DB dataset (Che et al., 2022), as well as its DAOD with the MACC (Monitoring Atmospheric Composition and Climate) simulation (Mukkavilli et al., 2019) and MODIS DB retrieved DAOD (Che et al., 2022). However, few studies were carried out to validate MERRA-2 near-surface dust concentrations.

Limited by a lack of ground-based near-surface observations, most validation studies of MERRA-2 component concentrations focus on a single site or a few sites, especially the dust component. For example, MERRA-2 OC, BC, sulfate concentration data sets have been validated against ground-based observations in China in Nanjing (Zhao et al., 2021) and Jingsha and Lin'an (Ma et al., 2021), Beijing (only BC) (Qin et al., 2019; Ou et al., 2022) and over northern India (OC and BC) (Soni et al., 2021). As for the dust component, daily MERRA-2 dust concentrations have been validated in Barbados (daily product) (Buchard et al., 2017), and Cayenne, Northern South America (Prospero et al., 2020).

Although there are relatively few ground-based observations, validation results still show daily and monthly MERRA-2 surface mass concentrations in the forms of PM2.5/10 or single components with relatively high accuracy. MERRA-2 near-surface component concentrations can be used for conversion to PM10 using the equation below (Provençal et al., 2017; Ma et al., 2021):

$$[PM10] = 1.375 \times [SO_4^{2-}] + 1.8 \times [OC] + [BC] + [DU_{10}] + [SS_{10}] \quad (1)$$

where $[SO_4^{2-}]$, [OC], [BC], $[DU_{10}]$, and $[SS_{10}]$ are concentrations of each aerosol component, namely sulfate, organic carbon, black carbon, dust, and sea salt aerosol, and the subscripts 10 indicates the particle diameter less than 10μm. Ma et al. (2021) derived from using the first three size bins for dust and sea salt aerosols. $[SO_4^{2-}]$ is multiplied by 1.375 under the assumption that SO_4 is fully neutralized by ammonium in the form of $(NH_4)_2SO_4$ (ammonium sulfate) and a scale factor of 1.8 for OC is included to take into consideration the organic compounds in the particulate organic matter. Equation 1 was developed for estimating MERRA PM10 over Europe (Provençal et al., 2017), which may be inappropriate for PM10 estimation over other regions. For example, Ma et al. (2021)

https://doi.org/10.5194/egusphere-2023-1710
Preprint. Discussion started: 13 September 2023

considered the increasing trend of nitrate which was a large proportion of aerosols over China and revised Eq.1 as:

$$[PM10] = 1.375 \times [SO_4^{2-}] + 1.29 \times [NO_3^-] + 1.8 \times [OC] + [BC] + [DU_{10}] + [SS_{10}] \quad (2)$$

where $[NO_3^-]$ is the concentration of nitrate. Considering that coarse mode aerosols take up 57%-71% of total aerosols over major cities (Chan et al., 2008), MERRA-2 PM10 for Australia was estimated using Eq.1.

In this study, the method developed by GMAO (Eq.3) using MERRA-2 3-D aerosol mass mixing ratios was used for PM10 estimation over Australia.

$$[PM10] = (1.375 \times [SO_4^{2-}] + [BCphobic] + [BCphilic] + [OCphobic] + [OCphilic] + [DU001] + [DU002] + [DU003] + 0.74 \times [DU004] + [SS001] + [SS002] + [SS003] + [SS004]) * AIRDENS \quad (3)$$

where the subscripts philic and phobic for [BC] and [OC] represent hydrophilic and hydrophobic BC and OC aerosols, respectively, the numbers after [DU] and [SS] indicate the 4 size bins, i.e. 001 to 004 represent the bins with radius from 001 for 0.1 to 1.0μm, 002 for 1.0 to 1.8μm, 003 for 1.8 to 3.0μm, and 004 for 3.0 to 6.0μm for dust, and similarly for 0.03 to 0.1μm, 0.1 to 0.5μm, 0.5 to 1.5μm, and 1.5 to 5.0μm for sea salt, and the AIRDENS means air density (https://gmao.gsfc.nasa.gov/reanalysis/MERRA-2/FAQ/#Q5)

2.3 MODIS DeepBlue AOD dataset

MODIS DB aerosol product provides nearly full global coverage of AOD, AE, and SSA datasets over EOS (Earth Observing System) years (from 2000 to the present) (Sayer et al., 2017). MODIS DB has been widely used for dust research over arid and semi-arid regions i.e., bright surfaces where the traditional dark target (DT) algorithm is not applicable. For example, Ginoux et al. (2012) analyzed the global distribution of dust sources and emissions using MODIS DB aerosol product, taking advantage of its coverage over bright surfaces and successful retrieval of AE and SSA together with AOD. Similarly with other aerosol products released by NASA like DT (Levy et al., 2013) and aerosol climate change initiative (aerosol_CCI) such as AATSR (Advanced Along-Track Scanning Radiometer) aerosol products (de Leeuw et al., 2015; Sundström et al., 2012; Kolmonen et al., 2016; Thomas et al., 2009), all L2 MODIS DB aerosol datasets in the latest C61 product were produced with a spatial resolution of 10km with all MODIS radiance data. In this study, MODIS DB aerosol product for Aqua from 2002-2020 was selected.

MODIS DB key parameters have been validated over Australia and globally, especially AOD. The MODIS DB

https://doi.org/10.5194/egusphere-2023-1710
Preprint. Discussion started: 13 September 2023

AOD dataset has been validated against AERONET data (Che et al., 2022; Sayer et al., 2019; Wei et al., 2019), inter-compared with other AOD products for MODIS, such as MAIAC and DT (Shaylor et al., 2022), and even evaluated with MERRA-2 AOD (Che et al., 2022) over Australia. These studies show that there is a high probability of data points (MODIS DB and AERONET) within EE lines, such as 67% points with an EE of $\pm(0.03 + 0.15\tau)$ (Che et al., 2022). The latest MODIS DB aerosol product limits AE values from 0 to 1.8, and in low AOD conditions AE is set to < 1.0 over bright surfaces and AE is fixed to 1.5 over vegetated surfaces (Sayer et al., 2013; Hsu et al., 2013). Sayer et al. (2019) tested the performance of MODIS AE in different conditions, including dust cases and fine mode cases. Over vegetated surfaces, MODIS DB AE was overestimated systematically with a broad range of error from 0.5 to 1 for dusty conditions, while over dry surfaces the performances of MODIS DB AE have improved in systematic overestimation but still a broad error range (Sayer et al., 2019). Therefore, dust detection by MODIS DB could be uncertain to some extent.

2.4 Gridded SILO monthly rainfall data

The SILO datasets developed by the Queensland government are aimed at providing long-term continuous point and full coverage gridded climate datasets for land areas of Australia from 1989 to the present (https://www.longpaddock.qld.gov.au/silo/). The full coverage gridded rainfall dataset at a temporal resolution of a day and a month were produced by interpolating BoM daily and monthly rainfall observations with a Kriging method (Jeffrey et al., 2001). Validation results show that the accuracy of SILO data is typically higher around areas with densely distributed BoM rainfall gauge sites (Jeffrey et al., 2001). Overall, except for parts of western Australia with few BoM rainfall sites SILO rainfall shows a high accuracy with an R^2 >0.8 over most of the Australian land (Jeffrey et al., 2001).

2.5 MODIS-MERRA (M&M) combined DAOD

DAOD has been successfully retrieved based on MODIS DB product by a coarse mode fraction (CMF) in Equation 4 (Ginoux et al., 2010, 2012; Pu and Ginoux, 2017):

$$CMF = 0.98\text{-}0.5098AE\text{-}0.05AE^2 \quad (4)$$

The early version of the MODIS DB DAOD dataset has been used for analyzing the global distribution of dust sources (Ginoux et al., 2012) and constructing a global DAOD climatology (Voss and Evan, 2020). The new version of MODIS DB DAOD dataset has been used for evaluating DAOD satellite remote sensing from GCMs and CALIOP, such as CMIP5 (Pu and Ginoux, 2018), MERRA-2 (Che et al., 2022), and CALIOP (Song et al.,

https://doi.org/10.5194/egusphere-2023-1710
Preprint. Discussion started: 13 September 2023

2021). In Australia, the MODIS DB DAOD dataset was validated against AERONET data and results show that 88% and 71% of data points for MODIS/Terra and MODIS/Aqua, respectively, fall within an EE of ($\pm0.05+0.15\tau$) (Che et al., 2022). Although studies have shown MODIS DB DAOD dataset is of high quality, there are still several factors limiting its applications to dust research in Australia. First, the data coverage of the MODIS DB DAOD dataset only includes obvious dust plumes. Secondly, MODIS DB AE retrievals have a broad range of errors over both bright and vegetated surfaces, especially systematical overestimations over vegetated surfaces (Sayer et al., 2019), causing non-negligible uncertainty in the MODIS DB DAOD dataset. Thirdly, AE was fixed in low AOD conditions (Sayer et al., 2013; Hsu et al., 2013). MERRA-2 aerosol reanalysis is expected to make up for these deficiencies.

A new DAOD dataset has been developed for Australia in this study using MODIS DB aerosol product and MERRA-2 aerosol reanalysis. Figure 2a shows MODIS DB AOD on 23rd October 2022 with hundreds of kilometers of dust plume in eastern Australia while the dust plume is seriously underestimated by MERRA-2 (Figure 2b) compared with MODIS BTD in Fig.2c. In order to take advantage of MODIS DB in catching dust plumes and MERRA-2 in spatial coverage, DAOD equals to MODIS DB DAOD when it is available, otherwise, DAOD equals to MODIS DB AOD multiplied by the ratio of MERRA-2 DAOD to total AOD. This is based on the assumption that the dust fraction in MERRA-2 is shown to have high accuracy with LIVAS (Gkikas et al., 2021) and AERONET (Che et al., 2022). Figure 2d shows that the final DAOD is capable of screening sea salt AOD over the Cape York Peninsula and has the same spatial coverage as MODIS DB AOD. Although Sayer et al. (2019) suggest that AE should be only used for discriminating coarse mode-dominated AOD from fine mode-dominated AOD qualitatively, a smoke plume (Fig.2d) over the Australian east coast was effectively removed from MODIS DB AOD.

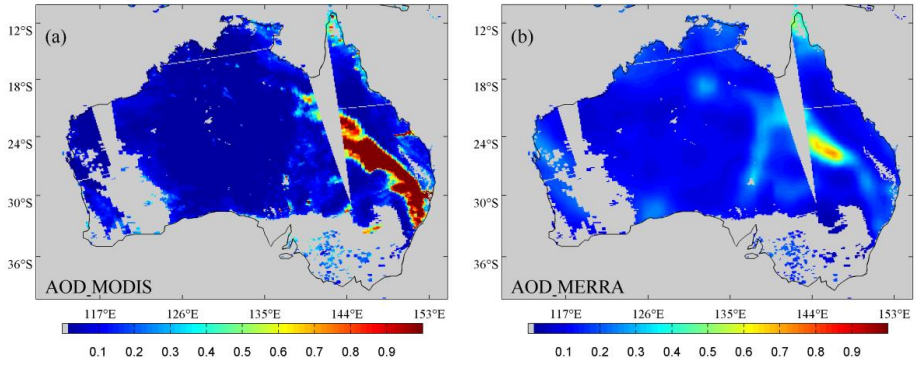

https://doi.org/10.5194/egusphere-2023-1710
Preprint. Discussion started: 13 September 2023

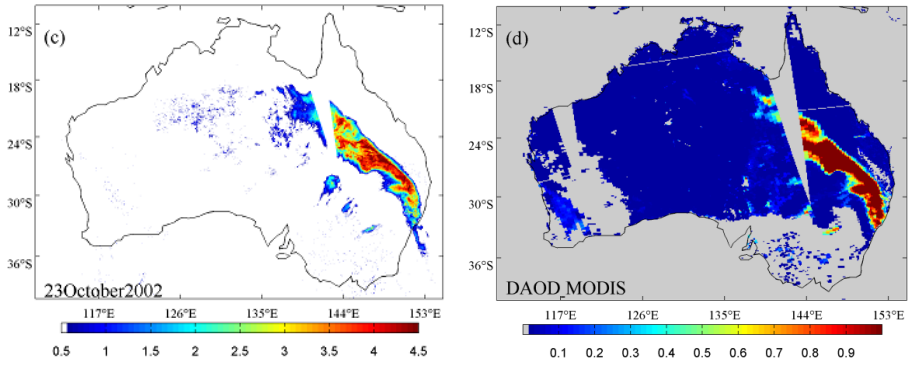

Figure 2: Development of DAOD using MERRA-2 and MODIS DB dataset. (a) MODIS DB AOD, (b) MERRA-2 AOD, (c) MODIS BTD, and (d) MERRA-MODIS combined DAOD (M&M).

3. Results

3.1 Validation of MERRA-2 surface mass concentration and DAOD

Figure 3 shows the validation result of MODIS (Aqua)-MERRA (M&M) combined DAOD over Australia from 2002-2020. The average AERONET DAOD for all collocated data points is only 0.03 for Australia. When AOD is low, remote sensing AOD retrievals are likely to be close to the margin of uncertainty and hence subject to large relative bias, especially over the arctic region (Mei et al., 2013b, a), Qinghai-Tibet Plateau (Che et al., 2018, 2016), and Australia (Che et al., 2022; Sayer et al., 2019). The ratio of RMSE (root mean square error) to the mean AERONET DAOD for MODIS-MERRA DAOD was 0.8, indicating that the uncertainty is close to MODIS-MERRA DAOD. The EE (expected envelope) that contains 68% of data points is $\pm(0.016 + 0.15\tau_{Aero})$ for MODIS-MERRA DAOD to AERONET DAOD over Australia. The intercept in EE is 0.016 is much smaller than for the MODIS DB AOD over Australia (0.03) (Che et al., 2022), suggesting a high level of accuracy of this MODIS-MERRA DAOD dataset with a smaller absolute error.

https://doi.org/10.5194/egusphere-2023-1710
Preprint. Discussion started: 13 September 2023

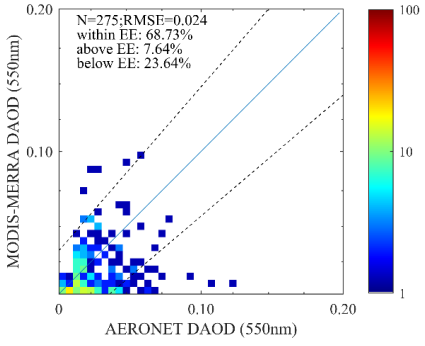

311

312 **Figure 3: Comparison of MERRA-MODIS DAOD with AERONET DAOD. The dashed lines denote an EE**
313 **of $\pm(0.016 + 0.15\tau_{Aero})$ which contains 68% of the data points. τ_{Aero} represents AERONET AOD.**

314

315 Figure 4 shows the validation results of MERRA-2 estimated monthly PM10 with ground-based observations at
316 62 AQMN stations for the period 2001-2020. There are 7438 data points in total for MERRA-2 PM10 validation
317 over eastern NSW. These selected PM10 observations are located downwind areas of inland dust sources such as
318 Lake Eyre, South Simpson lakes and the Channel country (O'Loingsigh et al., 2017). PM10 at these sites, therefore,
319 could represent dust activities in southeast Australia during dust seasons. The mean monthly PM10 for all data
320 points is 19.9μg/m^3, indicating a clear atmosphere over eastern NSW on average. When PM10 observations are
321 greater than 40μg/m^3, almost all the data points are below the 1-1 line, suggesting that MERRA-2 is incapable of
322 catching high PM10 events (dust or other pollutions). Due to the relatively dense spatial distribution, AQMN sites
323 are likely to observe the same dust events with similar PM10 observations and thus a similar extent of
324 underestimation. Time series plots (Fig.5) show similar severe underestimation in Newcastle (13.5μg/m^3 vs.
325 106.9μg/m^3), Randwick (12.4μg/m^3 vs. 84.7μg/m^3), and Wollongong (13.0μg/m^3 vs. 65.2μg/m^3) in September
326 2009 and Bathurst (18.9μg/m^3 vs. 104.8μg/m^3), Bulga (30.4μg/m^3 vs. 78.9μg/m^3), and Newcastle (37.1μg/m^3 vs.
327 50.8μg/m^3) in December 2019. In September 2009, a severe dust storm swept the Australian continent,
328 causing a jump in PM10 for overpass areas (Leys et al., 2011). High PM10 (higher than 300μg/m^3) lasted for
329 approximately 12 hours and reached as high as15388μg/m^3 at Bathurst. Similarly, high PM10 concentrations were
330 recorded at Bulga and Newcastle (Fig.5). Due to rainfall deficiency and high temperatures in November and
331 December 2019, NSW experienced the longest bushfire season when more than five million hectares were burned
332 (BBC News, 2020). The NSW AQMN stations, therefore, had recorded high PM10 concentrations during the
333 bushfire season. These underestimations by approximately 5 were also a major reason why the ground-based mean

https://doi.org/10.5194/egusphere-2023-1710
Preprint. Discussion started: 13 September 2023

PM10 (19.9μg/m^3) was higher than that of MERRA-2 (18.2μg/m^3). When PM10 is less than 20μg/m^3, data points show a slight bias of MERRA-2, and when PM10 is between 20μg/m^3 to 40μg/m^3, the bias in MERRA-2 reduces. This is shown by evenly distributed data points around 1-1 line but less association occurs between the two. Severe underestimations of MERRA-2 PM10 (Fig.5) show a strong seasonality at some sites like Albury and Bathurst in summer when PM10 is greater than 40μg/m^3. This suggests that MERRA-2 is very liky to underestimate dust severity in summer because dust events mainly occur in summer throughout the year in NSW (Che et al., 2022). In spite of the underestimations, MERRA-2 is capable of tracing the seasonal variations of PM10 at six sites with an r^2 value from 0.14 to 0.44. Overall, a RMSE is 10.8μg/m^3 for all monthly MERRA-2 and ground-based PM10 data.

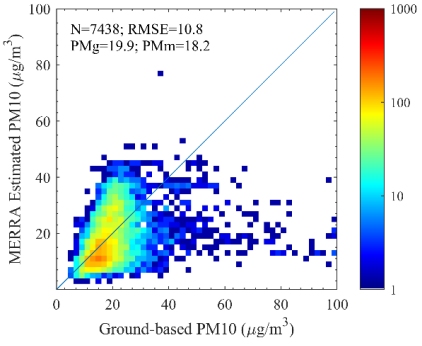

Figure 4: Comparison of monthly MERRA-2 estimated PM10 with ground-based PM10 observations at 62 AQMN stations.

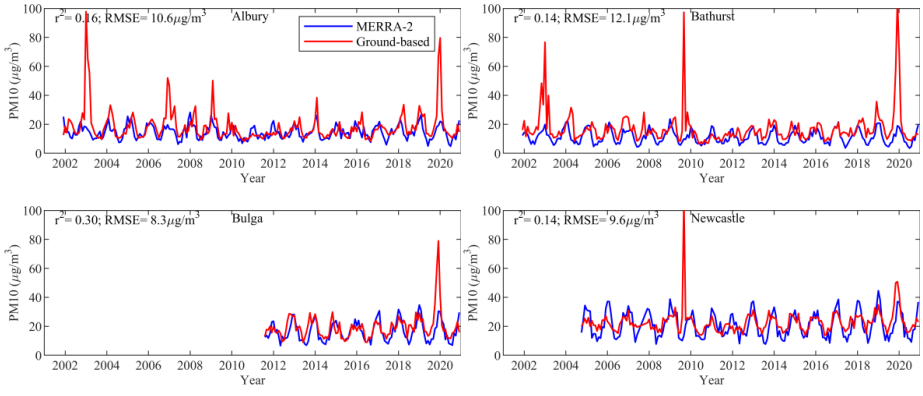

https://doi.org/10.5194/egusphere-2023-1710
Preprint. Discussion started: 13 September 2023

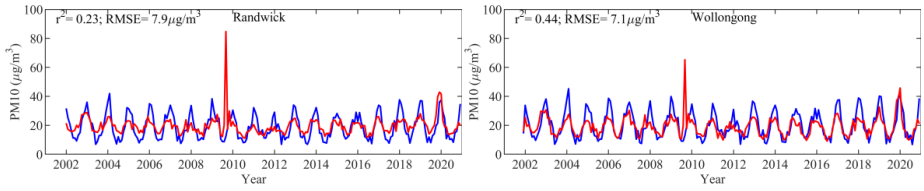

Figure 5: Time series for MERRA-2 estimated PM 10 with ground-based PM observations at 6 sites in NSW.

Figure 6 shows the relationships between MERRA-2 near-surface dust concentrations with horizontal visibility with a dust type based on SYNOP code at Charleville, Cobar, and Longreach. The relationships are similar at Charleville and Cobar in that MERRA-2 near-surface dust concentrations follow a power function relationship with horizontal visibility. The r^2 values for two sites of 0.44 and 0.39, respectively, also suggest a relatively robust relationship between the two datasets. At Longreach, a low r^2 value of 0.18 shows a weak relationship between MERRA-2 near-surface dust concentrations and visibilities. Longreach is known to bein a region of frequent local wind erosion activities with extensive tracts of clay soils in Eastern Australia (McTainsh et al., 1990). Alluvial sediments and sandy clays, therefore, would be important sources for local dust events in Longreach (Rust and Nanson, 1989; McTainsh et al., 1990). These clay aggregates exhibit lower optical extinction compared to fine clay. However, due to their larger mass, they can still contribute to a high concentration of dust near the surface in a high visibility condition. This explains why the r2 in Figure 6c differs from the other two. Previous studies showed that near-surface dust concentrations/total suspended particle concentrations agree statistically well with the visibility data (Baddock et al., 2014; Chepil and Woodruff, 1957; Shao et al., 2003; Tews, 1996) and visibility-defined DSI (O'Loingsigh et al., 2014), and horizontal visibility were often used for calculating dust concentrations (Leys et al., 2011; McTainsh et al., 2005). According to Shao et al. (2007), visibility observations are subjective and inaccurate; the sample size for regression equations is usually small; and dust concentrations are affected by dust particle size and humidity. Similar power function relationships between the two suggest the acceptable accuracy of MERRA-2 near-surface dust concentrations to an extent.

https://doi.org/10.5194/egusphere-2023-1710
Preprint. Discussion started: 13 September 2023

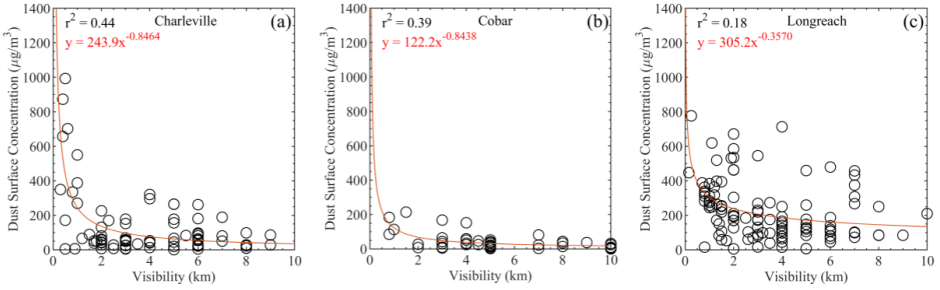

Figure 6: Relationships between BoM horizontal visibility observations of MERRA-2 dust surface mass concentrations.

Figure 7 shows dust pathways and sink areas for Australia as identified in previous studies. Bowler (1976) established the first dust pathways (Figure 7a) using trends of dust and sand dune movement during the period of intense dune building phases. Major dustfall areas lie mainly to the southeast and northwest of the Australian continent. Sprigg (1982) proposed a conceptual model (Figure7b) for describing how wind systems fed dust into the pathways identified by Bowler using measured wind run, wind direction, and wind speed in desert areas. Blewett (2012) adopted the dust pathways established by Bowler but provided a detailed classification of sand dunes and accurately confirmed dustfall in the southeast offshore area. Figure 7d shows MERRA-2 dust flux over Australia from 2002 to 2020. Compared to previous studies (i.e. Figure 7a-c), MERRA-2 flux quantitatively shows the mean dust pathways and dustfall areas for Australia, providing independent support to previous conceptual models.

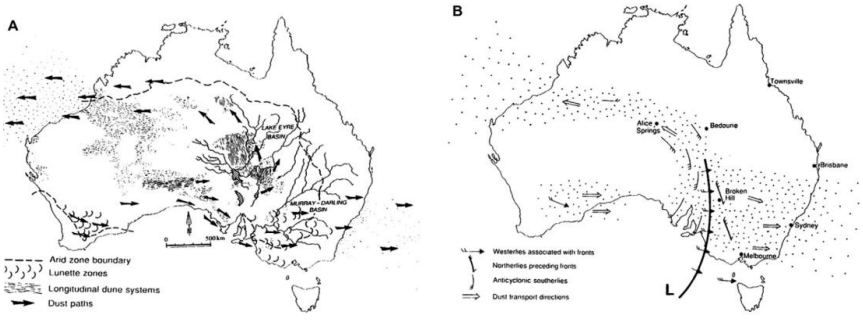

https://doi.org/10.5194/egusphere-2023-1710
Preprint. Discussion started: 13 September 2023

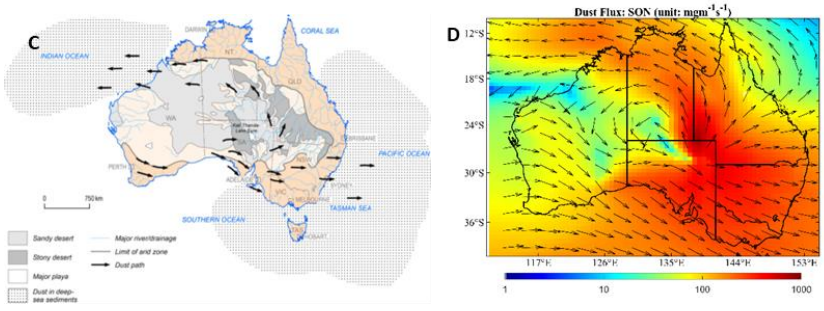

Figure 7: Comparison of dust pathways over Australia delineated in previous studies. (a) Bowler (1976), (b) Sprigg (1982), (c) Blewett (2012), and (d) mean dust flux based on MERRA-2 from 2002-2020.

3.2 Seasonal DAOD based on MODIS-MERRA, dust concentration and PM10 based on MERRA-2

Figure 8 shows the mean seasonal MODIS-MERRA DAOD over Australia from 2002 to 2020. Spring (Sep-Nov) and summer (Dec-Feb) are typically dust seasons in Australia, when DAOD is much higher than that in autumn (Mar-May) and winter (Jun-Aug). This seasonal pattern is consistent with that shown by monthly dust event frequency based on synoptic observations (McTainsh et al., 1998). As dust activities would normally last until March in southeastern Australia (McTainsh et al., 1998), DAOD in this area is relatively high compared to that in Western Australia (Fig. 8b). High rainfall may inhibit occurrences of dust events, therefore, Figure 8c shows low DAOD for most of Australia in winter.

High DAOD is shown over dust source areas and along main pathways. Dust and sand particles originated from the inland area (around the Lake Eyre Basin), and were transported along two main dust transport pathways to the north and southeast (Bowler, 1976; De Deckker, 2019; McGowan et al., 2000; Sprigg, 1982; Strong et al., 2011). In spring (Figure 8d), high DAOD regions are mainly concentrated around the Lake Eyre Basin in southeastern Australia, and in the southwest of Western Australia. Fig. 8d shows that the flux with dust entrained from the source region in Central Australia to the southeast is so far the strongest over the Australian continent. DAOD and dust flux are consistent with each other and both reflect the major dust pathway in southeastern Australia. High DAOD can be also found in the southwest of Western Australia, which has been identified as the starting point of the major pathways flow in the south in previous studies (Sprigg, 1982). Due to onshore winds, high DAOD around this region is very likely to be generated from local dust sources. Also, DAOD in spring is much higher than in other seasons in this region. In summer (Figure 8a), the highest DAOD regions were found in the main

https://doi.org/10.5194/egusphere-2023-1710
Preprint. Discussion started: 13 September 2023

pathway to the north as highlighted with a red box, and around the center of the Lake Eyre Basin. The high DAOD region in the north of NT and QLD is in the main pathway, with a spatial pattern consistent with prevailing wind directions. Another region with high DAOD in the middle of QLD shows a different spatial pattern with MERRA-2 dust flux, which may be caused by differences in data coverage between MODIS DB and MERRA-2 datasets. The second highest DAOD regions are concentrated around the southeast dust pathway in NSW. Meanwhile, dust flux for these regions is much lower than those for northern regions. In autumn (Figure 8b), DAOD is an extension of that in summer that DAOD shows a very similar spatial pattern to that in summer but lower in value. In regions with high DAOD, DAOD distribution is consistent with that of dust flux (i.e., high DAOD corresponds to large dust flux). In winter, dust emissions in the center of Lake Eyre Basin are the smallest and DAOD is the lowest among the four seasons. Dust is mainly transported to the east coast of Australia, deposited in eastern Australia and the ocean aresa to the southeast and northwest.

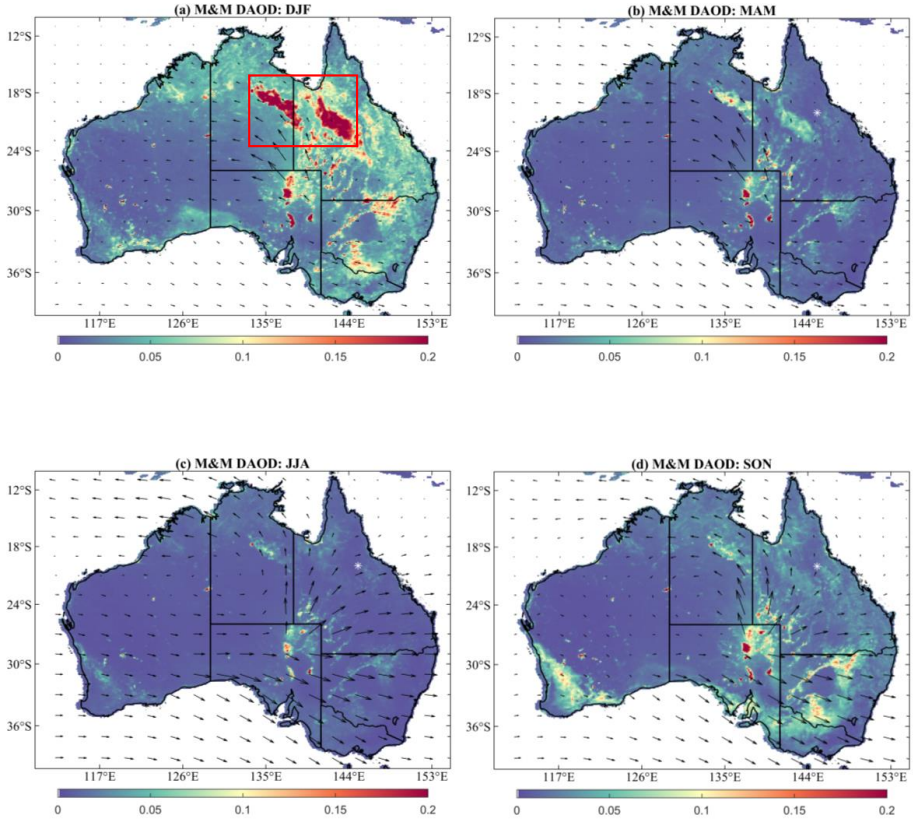

https://doi.org/10.5194/egusphere-2023-1710
Preprint. Discussion started: 13 September 2023

Figure 8: Seasonal MERRA-MODIS DAOD from 2002-2020. (a) Sep-Nov, (b) Dec-Feb, (c) Mar-May, (d) Jun-Jul. Arrows represent dust flux (unit: kg/m·s) with the direction and magnitude.

Figure 9 shows mean seasonal near-surface dust concentrations and PM10 based on MERRA-2, and the ratio of the two for Australia. The highest near-surface dust concentrations are mainly distributed over the Lake Eyre Basin which is the largest natural dust source in Australia, while high concentrations from 50 to 100μg/m^3 are found around the Lake Eyre Basin, Great Victoria Desert, and Nullarbor Plain in four seasons (See Figure.9a, d, g, and j). In other regions, near-surface dust concentrations typically are less than 50μg/m^3 and the concentration decreases towards the coastline. Low concentrations of less than 20μg/m^3 of dust can be found over the ocean, particularly the Indian Ocean in the northwest. MERRA-2 PM10 (See Figure 9b, e, h, and k) shows that the spatial distribution is similar to that of the near-surface dust concentrations over the continent. Differences between the two mainly occur in the offshore areas due to the influence of sea salt aerosols and carbonaceous aerosols in the north in spring (Yang et al., 2021). Spatial distributions of dust concentration and PM10 are similar because PM10 accounts for the majority of dust particles in inland Australia (Figure 9c, f, I, and l). A high ratio of dust concentration over PM10 of over 0.7 is mainly found in inland areas and the ratio decreases towards the coastline which is consistent with that coarse particles settle out of suspension more quickly compared to finer particles (Fryrear et al., 1991). It should be noted that four states in eastern Australia are affected relatively less by dust than other regions from the perspective of the ratio of dust to PM10. The least affected states are VIC (higher than 0.2), NSW (0.3), and QLD (higher than 0.3), respectively.

The center of the Lake Eyre Basin emits most of the dust and largely determines the distribution of dust over the entire continent. The near-surface dust concentration is over 300μg/m^3 in the center of the Lake Eyre Basin in spring and summer while it decreased to approximately 200μg/m^3 in autumn and winter. The high concentration is related to dust activities in the dust source areas. With frequent dust activities (in addition to high dust concentrations over the center of the Lake Eyre Basin) the region with a dust concentration over 50μg/m^3 in summer and spring is much higher than that in autumn and winter, especially the Great Victoria Desert and Nullarbor Plain. The near-surface dust concentrations over two major dust pathways changed a little with season compared to that over the main dust source areas in the center of the continent. Relatively high concentrations of near-surface dust is found to the north in the four seasons compared to that along the dust pathway to the southeast.

https://doi.org/10.5194/egusphere-2023-1710
Preprint. Discussion started: 13 September 2023

455 The wind systems responsible for dust pathways as described by Sprigg (1982), explain that pre-frontal anti
456 cyclonic northerly winds are responsible for the main dust pathway in the south. High dust concentrations are,
457 however, not found in the main dust deposition area in the southeast.

458

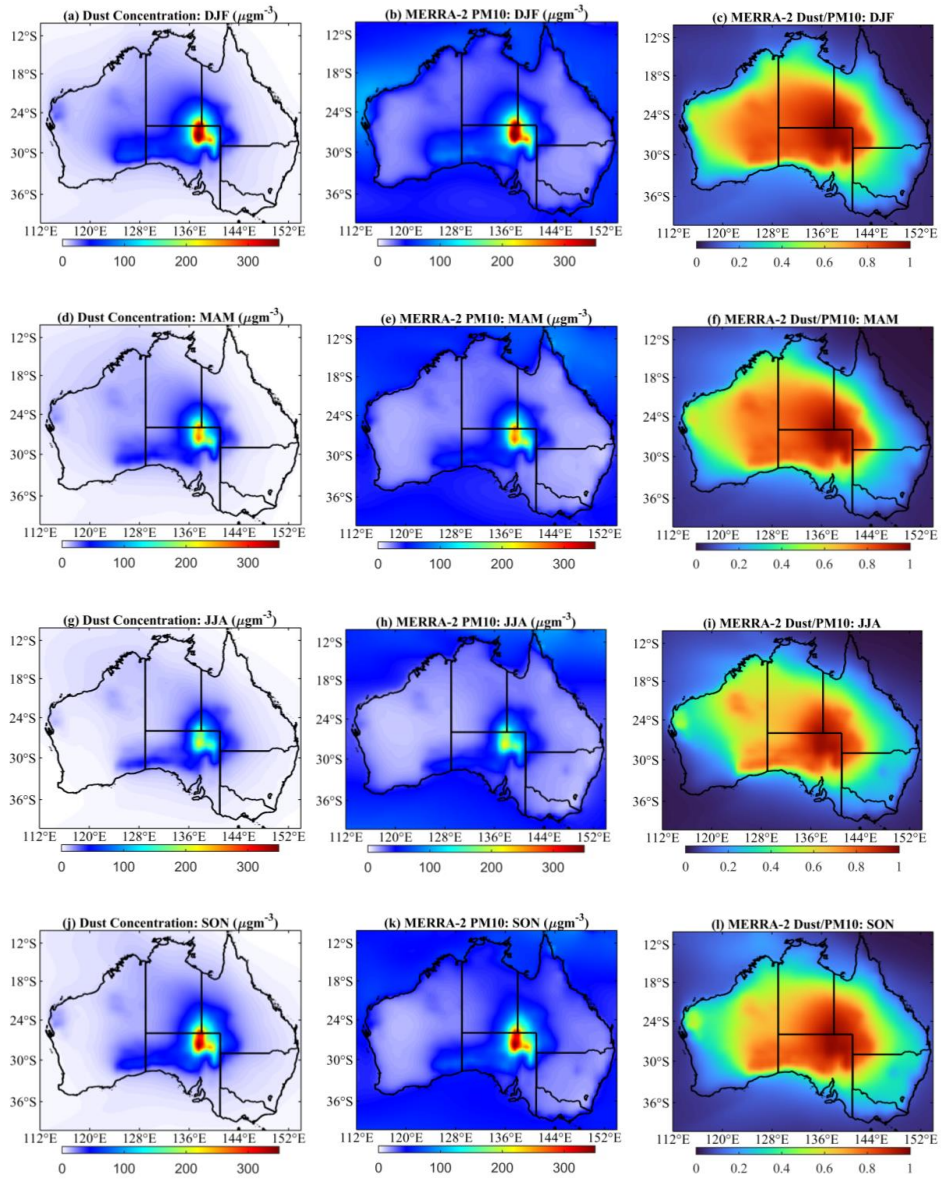

459

460

461

462 **Figure 9: Seasonal MERRA-2 near-surface dust concentration in (a) Dec-Feb, (d) Mar-May, (g) Jun-Jul,**
463 **and (j) Sep-Nov from 2002-2020; Seasonal MERRA-2 PM in (b) Dec-Feb, (e) Mar-May, (h) Jun-Jul, and**

https://doi.org/10.5194/egusphere-2023-1710
Preprint. Discussion started: 13 September 2023

(k) Sep-Nov from 2002-2020; and the ratio of MERRA-2 near-surface concentration to MERRA-2 PM10 in (c) Dec-Feb, (f) Mar-May, (i) Jun-Jul, and (l) Sep-Nov from 2002-2020.

3.3 Dust loading budget in the Australian continent

Figure 10 shows the directions of dust flux using MERRA-2 dust flux datasets. The colors of the coastline indicate whether dusts are exported (red) or imported (blue). As the "loneliest" inhabited continent, Australia is located far away from other continents, with the largest natural dust source in the southern hemisphere , the Lake Eyre Basin, and thus regarded as a main dust source exporting dust. However, the blue border shows that areas of import can occur along the west, north, and south coasts. Along the north coast, exported dust from QLD could be transported back to the Cape York Peninsula, part of this dust would travel on to Arnhem Land and even travel back to the continent. This recirculated dust cannot be defined as imported dust because it originated from the Australian continent, was transported over the sea and back onto the continent. A similar situation can be found on the coastline in South Australia where dust originated from the continent and was transported outwards from the Nullarbor Plain, across the Spencer Gulf and back to South Australia and VIC. Different from these two situations, dust imported from the west coast is very likely to be from remote dust sources in South Africa. Firstly, MERRA-2 dust flux doesn't show dusts exported from the northwest coast are transported back to the continent. Secondly, dust originating from the Mallee region is unlikely to be transported to the west coast crossing the Pacific Ocean (Bhattachan and D'Odorico, 2014). Thirdly, the southwesterly winds are key to transporting dust from South Africa to Western Australia due to their similar latitudes (Torre et al., 2022). The dust imported from 20°S to 36°S is therefore regarded as the only imported dust from an external source for Australia in this study.

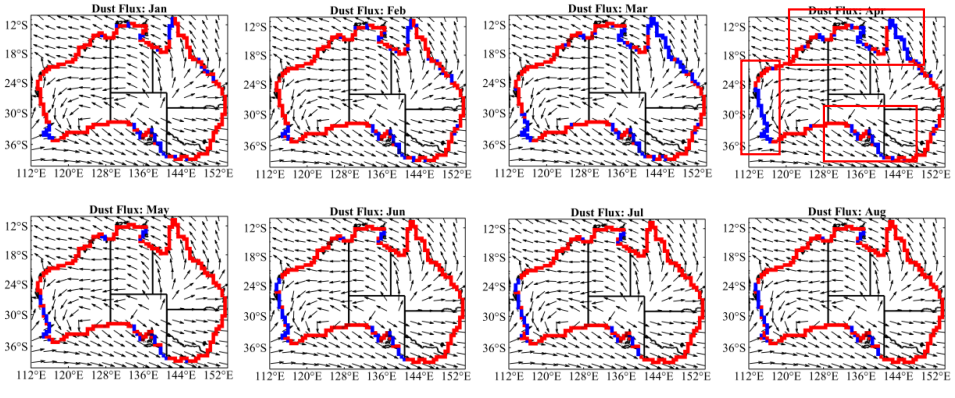

https://doi.org/10.5194/egusphere-2023-1710
Preprint. Discussion started: 13 September 2023

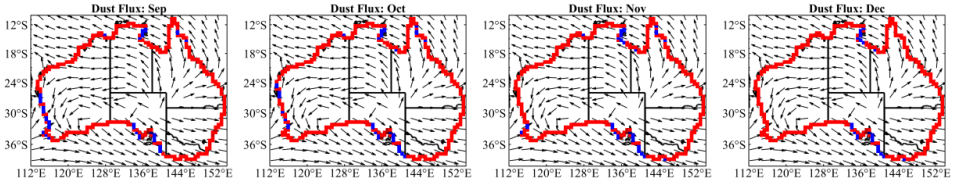

Figure 10: Directions of dust flow in each month. Blue and red borders indicate imported and exported dust, respectively.

Figure 11 shows the annual dust budget for Australia from 1980 to 2020 using MERRA-2 aerosol reanalysis. The green line shows the annual total dust emission, and suggests a slight decreasing trend over the past 42 years. Overall, the Australian continent emits on average 41.84±3.10 Mt/yr into the atmosphere from 1980 to 2020, of which 19.63±2.48 Mt/yr is exported from Australia, 1.34±0.55 Mt/yr imported from non-Australia dust sources, and 23.56±2.99 Mt/yr deposited over the land area. The average annual dust emission over each decade from the 1980s to the 2010s are 43.12 Mt/yr, 42.63 Mt/yr, 41.36 Mt/yr, and 39.99 Mt/yr, respectively, showing an overall decreasing trend on a decade basis. The dust emission peaks are at 48.9 Mt/yr and 48.0 Mt/yr in 1990 and 1996, respectively. Although most of Australia was in drought during these two years, the dust storm index based on visibility data and weather codes for these two years is around the average from 1965 to 2009 at 180 long-term stations (O'Loingsigh et al., 2014). The DSI for these two years was around the average from 1960 to 2000 at both inland and coastal stations (Ekström et al., 2004). Since 1996, sharp reduction of 10.2 Mt/yr occurred in dust emission in 1997 and the change from 1998 to 2020 is relatively small (with a standard deviation of 2.27Mt/yr excluding 2010) to that for the period from 1980 to 1997. Dust emission reached its minimum at 31.6Mt/yr in 2010. This may be strongly related to high rainfall in Australia in 2010 when the average rainfall was 687.3mm, which is only about 17mm lower than the highest rainfall of 710.6mm in 2000 during the period of 41 years (rainfall data can be found at http://www.bom.gov.au/web01/ncc/www/cli_chg/timeseries/rain/0112/aus/latest.txt). The black dashed line in Figure 11 represents the net dust export that equals to the dust leaving the Australian coastline (total net export) minus that imported from west coastal (total net import) line from 20°S to 36°S on an annual basis. The blue line shows the total annual dust deposition over the continent, and was calculated using the mass balance equation (Eq.5). The annual dust deposition shows a similar general trend to dust emission while opposite trend to dust export from 1980 to 2020. As annual dust deposition decreasesthe dust export increases (from 1980 to 2009). After a low value (16.2 Mt/yr and 16.8 Mt/yr) for both dust deposition and export in 2010,

https://doi.org/10.5194/egusphere-2023-1710
Preprint. Discussion started: 13 September 2023

the annual dust export began to decrease, while annual dust deposition started to increase from 2010 to 2020. On a decade basis, the annual dust export reached its maximum (22.2Mt/yr) in the 2000s, while annual dust deposition reached the minimum of 21.1Mt/yr over the same period. During this decade, dust exported from Australia was the closest to dust imported.

$$E + I = X + D \tag{5}$$

where E, I, X, and D represent annual dust emission, dust import, dust export, and dust deposition, respectively. E was calculated using MERRA-2 dust emission datasets for all particle bins, I and X were calculated using MERRA-2 dust flux datasets. With equation 5, D can be evaluated.

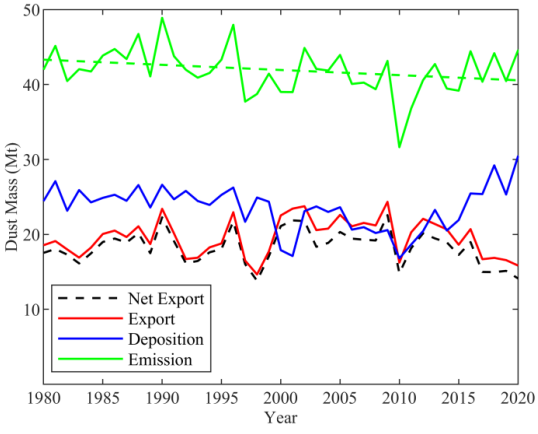

Figure 11: Annual dust budget for Australia. Green: annual dust emission, green dashed: trend of annual dust emission, red: dust export, blue: dust deposition, and black dashed: net dust export (net export-, export-, deposition is the difference between emission and net export).

Table 1 presents details of the annual dust loading for Australia in terms of clay and silt. Clay is a fine particle, traditionally ranging from 0.1~1.0μm in radius, which corresponds to MERRA-2 dust bin001. Silt is a much coarser particle with a broad size range of roughly 1.0μm to 25.0μm in radius. Although in the MERRA-2 dataset, the sum of dust bin002 to bin005 only covers 1.0μm to 10μm, in this study, the sum of dust bin002 to bin005 was regarded as silt particles. Generally, clay accounts for 6.63±0.10% of the total dust emission in Australia and silt for 93.37±0.10%. As for dust sedimentation, almost all sediment (99.57±0.02%) is from coarse silt particles, indicating that fine particles are more likely to be transported and exported from the Australian continent.

https://doi.org/10.5194/egusphere-2023-1710
Preprint. Discussion started: 13 September 2023

Table 1. Annual dust budget for Australia in terms of clay and silt.

	particle size (Radius)	Emission (Mt/yr)	Dry (Mt/yr)	Wet (Mt/yr)	Sedimentation (Mt/yr)
Total	0.1~10.0μm	41.84±3.10	2.65±0.35	4.48±0.76	19.76±1.17
Clay	0.1~1.0μm	2.78±0.24	0.36±0.05	0.55±0.10	0.09±0.01
		6.63±0.10%	13.42±0.46%	12.27±0.28%	0.62±0.04%
Silt	1.0~10.0μm	39.07±2.86	2.30±0.30	3.93±0.67	19.68±1.17
		93.37±0.10%	86.58±0.46%	87.73±0.28%	99.57±0.02%

4. Discussion

There are differences in the spatial distribution of dust activity in Australia based on different indicators from multiple data sets. Meteorological visibility-based dust event database (DEDB) and DSI were often used to indicate the level of dust activity in Australia over the past several decades (Ekström et al., 2004; McTainsh et al., 2011a; McTainsh and Pitblado, 1987; McTainsh et al., 1990, 1989b; McTainsh and Boughton, 1993; McTainsh et al., 1998, 1989a, 2011b; O'Loingsigh et al., 2014). Although these indicators are quite capable of identifying the type of dust events and the dust source areas, dust severity using meteorological observations is limited because 1) definitions of dust events change over time, 2) only the most-coded type was recorded, 3) there is inconsistency in records at different meteorological sites, 4) synoptic observations are subjective, 5) BoM sites are sparse in remote areas (McTainsh et al., 2011a; McTainsh and Pitblado, 1987; O'Loingsigh et al., 2010; Strong et al., 2011). DEDB/DSI can be a valuable reference dataset for assessing remote sensing and reanalysis products due to the long-term coverage and distribution of BoM weather stations. The spatial distribution of dust activities identified with DEDB/DSI differs from that based on M&M and MERRA-2, including:

1) M&M DAOD shows that dust activities are most severe over the main dust source area, the Lake Eyre Basin, and along major dust pathways over eastern Australia from 2002 to 2020 while the atmosphere is relatively clean over Western Australia. DEDB/DSI (McTainsh et al., 2011a) and MERRA-2 near-surface dust concentration show not only high dust concentration over dust source areas in central Australia but also elevated dust concentration over downwind areas in the southeast and northwest of Australia. The main difference between the latter two is that MERRA-2 is able to quantify dust activity with near-surface dust

https://doi.org/10.5194/egusphere-2023-1710
Preprint. Discussion started: 13 September 2023

concentrations and its variation over the Lake Eyre Basin, Nullarbor Plain, and downwind areas; on the contrary, DEDB/DSI can only indicate dust activity at a few sites.

2) Although M&M DAOD shows high dust concentrations over eastern Australia in spring and summer, its spatial pattern is dissimilar to that of DEDB/DSI. The dusty season is spring for the northern part of Australia and summer for the southern part using DEDB (McTainsh et al., 1998), while two regions with high DAOD were found over northern Australia in summer. In another study based on MODIS DB aerosol product conducted by Ginoux et al. (2012), these two regions (the Barkly Tableland and the lee side of the Great Dividing Range) were found in spring, which differs from this study but coincides with the work of McTainsh et al. (1998). This is probably because 1) McTainsh et al. (1998) uses meteorological data from 1960-1987 while the MODIS DB data from 2003 to 2009 (Ginoux et al., 2012) and MODIS DB data from Aqua from 2002 to 2020 has been used in this study, 2) MODIS DB shows much higher AOD over these two regions than MAIAC AOD (Shaylor et al., 2022), and MODIS DB retains high AOD for thick dust plumes (Che et al., 2022). For example, for the most severe two dust storms over Australia in the last twenty years, MODIS DB shows high AOD retrievals for the main dust plumes, which are even higher than 3.0, and the closest AERONET AOD to satellite Aqua overpass time is much less than MODIS DB (Che et al., 2022). This difference also indicates that more validation is still needed for MODIS DB aerosol products in Australia.

3) Another difference between M&M dataset with DEDB/DSI and MERRA-2 is that the former shows high level of dust activity over the southwest of Western Australia in spring and summer while the latter two don't.

Although the MERRA-2 dust dataset is well-constrained globally and even used as reference data to validate output from other models (Wu et al., 2020), the dust emission simulation for Australia in different studies vary considerably (Chen et al., 2022). MERRA-2 adopts the dust emission scheme proposed by Ginoux et al. (2001), which is based on soil wetness and surface wind speed. Areas of dust emission are located where rainfall is low, especially below 150mm/yr (Fig.12). Discrepancy in the dust emission scheme may lead to different dust simulation outputs. Wu et al. (2020) compared MERRA-2 dust emission for different regions with 15 CIMP models and shows that the annual dust emission for Australia varies from 0.6 Mt/yr to 2278 Mt/yr and only three out of 15 models (one with Ginoux's dust emission scheme) output similar dust emission to MERRA-2. Chen et al. (2022) compared annual dust emissions in nine studies and find that the annual dust emission for Australia in these studies varies within a relatively small range from 37 Mt/yr to 163 Mt/yr. Moreover, estimates of dust loading

https://doi.org/10.5194/egusphere-2023-1710
Preprint. Discussion started: 13 September 2023

based on ground-based data for a single dust event reveal that MERRA-2 may underestimate dust emission in Australia. McTainsh et al. (2005) point out that published studies are very likely to overestimate dust loading under the assumption that dust concentration is uniform from the bottom to the top and recalculated dust loadings for dust storms on 8 February 1983 Melbourne, 20–30 May 1994 South Australia, 1 December 1987, and 23 October 2003, which were 1.23Mt, 3.3-6.4Mt, less than 3.35-4.85Mt, and 3.35-4.85Mt, respectively. These single dust event over a region produced close or even more dust than MERRA-2 monthly total dust emission from the entire Australia (3.58Mt, 2.35Mt, 4.76Mt, and 5.49Mt for corresponding months), indicating that MERRA-2 might underestimate dust emission in Australia.

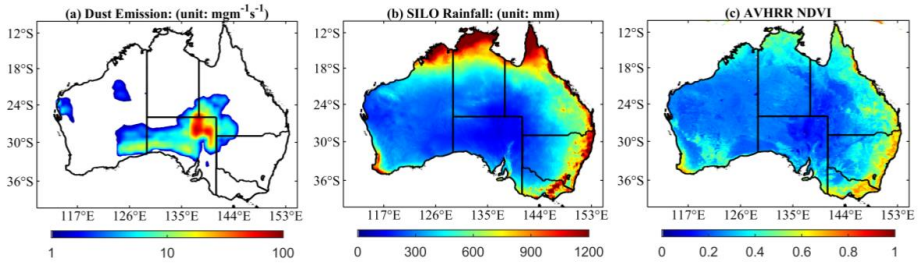

Figure 12: Mean annual MERRA-2 dust emission (a), SILO mean annual rainfall, and (c) AVHRR NDVI from 1982 to 2019.

There is an inconsistency between dust emission and dust wet/dry deposition in Australia. This is because the rate aerosol deposition based on MERRA-2 is be affected by its incremental update procedure and the bias in the underlying aerosol model (Wu et al., 2020). The average dust emission (41.84Mt/yr.) plus dust import (1.34Mt/yr.) is much higher than the averaged dust dry/wet deposition (7.13Mt/yr.) plus dust export (19.63Mt/yr.) from 1980 to 2020. The difference of approximately 16.4Mt/yr. or 38% suggests that the MERRA-2 dust deposition needs to be adjusted to balance with dust emission. If dust sedimentation replaces dust deposition in the dust balance, there is still a difference of 3.80Mt/yr., indicating that equation 5 still doesn't hold.

The long-term broad scale of reanalysis and remote sensing are most useful for studying climatic controls over dust activities. In the early 1990s, Yu et al. (1992, 1993) investigated the impact of rainfall in dust source areas in the previous autumn on dust event days in the following summer. At a much larger scale McTainsh et al. (1998) find that climatic drivers, i.e. wind run and soil moisture, to dust storm frequencies in the north and south parts of eastern Australia work differently in the dust seasons using BoM meteorological observation data. Although

https://doi.org/10.5194/egusphere-2023-1710
Preprint. Discussion started: 13 September 2023

McTainsh et al. (1998) state that the real control upon dust storms is soil moisture and associated surface vegetation rather than rainfall, Dust emission shows a similar spatial pattern with rainfall (Fig. 12). The statement by McTainsh et al. (1998) about climatic drivers is based on BoM meteorological records in Eastern Australia. Their conclusion may not apply to Central Australia predominated by long-term low rainfall and sparsely distributed vegetation. On the basis of McTainsh et al. (1998), Ekström et al. (2004) investigated the relationship between Australian dust storms and synoptic pressure distributions and find that spring-summer dust storms over central and southern Australia are most likely controlled by cold fronts with no precipitation and the summer-autumn dust storms are most likely controlled by the driest period of the year. Speer (2013) finds that westerly-induced dust storms that transport dusts to the east coast tend to occur during El Nino years and positive and negative phases of the southern annular mode (SAM). With remote sensing products, Yu and Ginoux (2021) assess how ENSO and the Madden-Julian Oscillation (MJO) influence dust activities in Australia. They further reveal that during MJO phases dust activities are impacted by anomalies in convection and wind due to MJO and soil moisture and vegetation due to ENSO.

5. Conclusion

On the basis of Che et al. (2022), this paper built a DAOD dataset based on MODIS DB and MERRA-2 aerosol datasets. Additionally, it has validated the MERRA-2 near-surface dust concentration, MERRA-2 estimated PM10, major dust pathways, MERRA-2-MODIS combined DAOD (M&M) with collected ground-based data and with these data sets analyzed the spatial and temporal distribution of dust activity over Australia from 1980-2020. The M&M DAOD dataset was found to be of acceptable accuracy in Australia compared with AERONET data. M&M DAOD contributes to long-term dust research in Australia. A power law relationship (similar to previous studies) has been found between MERRA-2 hourly near-surface dust concentration and BoM manual horizontal visibility at three sites in eastern Australia. Monthly MERRA-2 estimated PM10 show similar variations with AQMN ground-based PM10 observations with an r^2 value from 0.14 to 0.44 at 6 selected sites; however, MERRA-2 PM10 is not sensitive to low PM10 in winter, peaks in summer and is very likely to miss extreme high monthly PM10 values. MERRA-2 flux in MERRA-2 aerosol reanalysis shows similar general dust pathways (Bowler, 1976; Sprigg, 1982) suggesting that both early simulations and MERRA-2 are all reliable in identifying dust pathways. Moreover, MERRA-2 further provides quantitative details on dust concentration and fluxes in a spatially consistent manner.

https://doi.org/10.5194/egusphere-2023-1710
Preprint. Discussion started: 13 September 2023

Dust events over Australia are shown to be concentrated in the north and southeast in spring (Sep-Nov), occur anywhere to the east in summer, with the dust season finishing in autumn (based on M&M DAOD). Three main dust regions have been identified. These includethe southwest of Western Australia, and the north and south of eastern Australia. Dust events over the southwest of Western Australia only span two months, starting in September and reaching their peak in October. Dust events to the north of eastern Australia start in October, gradually reaching a peak in December and January, ending in April. Dust events for the north of eastern Australia start in November, with low levels of activity in December, reaching a peak in January and gradually end in April.

Near-surface dust concentrations were found to be the highest (over 200μg/m^3) over the center of Lake Eyre Basin, and weakened radially according to distance from the center, decreasing to below 20μg/m^3 along the two main pathways to the southwest and northeast. The dust pathway in the southeast shows lower near-surface dust concentrations than northest, coinciding with the fact that dust entrained in central Australia is hardly transported to the east coast (Speer, 2013). This is also shown by the ratio of near-surface dust concentration to PM10, where high values are concentrated around central Australia and relatively low ratios (below 0.5) are found in eastern Australia.

Total dust emission was estimated to be 40 Mt (mega-tonnes) per year over the period 1980-2020, of which nearly 50% was deposited on land; the rest as net export from the Australian continent. In the 2000s, more dust was exported than over other periods, 22.2 Mt/yr vs. 18.7 Mt/yr, and the closest to dust deposition (21.1 Mt/yr, the lowest); however, approximately 24 Mt/yr was deposited over the land area over other periods. Among these particles, 6.63±0.10% (2.78±0.24Mt/yr) of emission was clay particles and almost all dust sedimentation (99.57±0.02%) consisted of silt. This indicates that exported dust from Australia is mainly composed of fine particles (clay). Additionally, dust import was identified from the north, south, and west coastlines using MERRA-2 flux data. Only dust across the coastline in southwest of Western Australia was genuinely exported from other continents while other imported dusts are sourced and recycled from exported dusts from Australia across the north and south coastlines.

Data availability. The MERRA-2 and MODIS DB products are publically available from

https://doi.org/10.5194/egusphere-2023-1710
Preprint. Discussion started: 13 September 2023

https://search.earthdata.nasa.gov/search. The PM10 data can be downloaded from http://www.environment.nsw.gov.au/AQMS/search.htm and the hourly horizontal visibility is available from the Australian Boreau of Metorology. The SIlO rainfall data can be accessed from https://www.longpaddock.qld.gov.au/silo/gridded-data/.

Author contributions. Yahui Che: Term, Conceptualization, Data curation, Methodology, Software, Visualization, Investigation, Writing – original draft, preparation. Bofu Yu: Supervision, Writing – review & editing. Katherine Parsons: Writing – review & editing."

Conflict of interest statement. The authors declare that they have no known competing financial interests or personal relationships that could have appeared to influence the work reported in this paper.

Acknowledgement. We are thankful to the Australian Bureau of Meteorology for observing and maintaining the horizontal data. The first author acknowledges Griffith University for the financial support provided through the Griffith University International Postgraduate Research Scholarship (GUIPRS) and the Griffith University Postgraduate Research Scholarship (GUPRS).

https://doi.org/10.5194/egusphere-2023-1710
Preprint. Discussion started: 13 September 2023

References

Ackerman, S. A.: Using the radiative temperature difference at 3.7 and 11 μm to tract dust outbreaks, Remote Sens. Environ., 27, 129–133, https://doi.org/10.1016/0034-4257(89)90012-6, 1989.

Angstrom, A.: Solar and terrestrial radiation. Report to the international commission for solar research on actinometric investigations of solar and atmospheric radiation, Q. J. R. Meteorol. Soc., 50, 121–126, https://doi.org/10.1002/qj.49705021008, 1924.

Baddock, M. C., Bullard, J. E., and Bryant, R. G.: Dust source identification using MODIS: A comparison of techniques applied to the Lake Eyre Basin, Australia, Remote Sens. Environ., 113, 1511–1528, https://doi.org/10.1016/j.rse.2009.03.002, 2009.

Baddock, M. C., Strong, C. L., Leys, J. F., Heidenreich, S. K., Tews, E. K., and McTainsh, G. H.: A visibility and total suspended dust relationship, Atmos. Environ., 89, 329–336, https://doi.org/10.1016/j.atmosenv.2014.02.038, 2014.

BBC News: Australia weather: How much rain did it take to put out NSW fires?, 2020.

Bhattachan, A. and D'Odorico, P.: Can land use intensification in the Mallee, Australia increase the supply of soluble iron to the Southern Ocean?, Sci. Rep., 4, 6009, https://doi.org/10.1038/srep06009, 2014.

Blewett, R.: Shaping a Nation:A Geology of Australia, Commonwealth of Australia and ANU-E Press, Canberra, 2012.

Bowler, J. M.: Aridity in Australia: Age, origins and expression in aeolian landforms and sediments, Earth-Science Rev., 12, 279–310, https://doi.org/10.1016/0012-8252(76)90008-8, 1976.

Buchard, V., Randles, C. A., da Silva, A. M., Darmenov, A., Colarco, P. R., Govindaraju, R., Ferrare, R., Hair, J., Beyersdorf, A. J., Ziemba, L. D., and Yu, H.: The MERRA-2 aerosol reanalysis, 1980 onward. Part II: Evaluation and case studies, J. Clim., 30, 6851–6872, https://doi.org/10.1175/JCLI-D-16-0613.1, 2017.

Bullard, J., Baddock, M., McTainsh, G., and Leys, J.: Sub-basin scale dust source geomorphology detected using MODIS, Geophys. Res. Lett., 35, 15404, https://doi.org/10.1029/2008GL033928, 2008.

Chan, Y.-C., Cohen, D. D., Hawas, O., Stelcer, E., Simpson, R., Denison, L., Wong, N., Hodge, M., Comino, E., and Carswell, S.: Apportionment of sources of fine and coarse particles in four major Australian cities by positive matrix factorisation, Atmos. Environ., 42, 374–389, https://doi.org/10.1016/j.atmosenv.2007.09.030, 2008.

Che, Y., Xue, Y., Mei, L., Guang, J., She, L., Guo, J., Hu, Y., Xu, H., He, X., Di, A., and Fan, C.: Technical note: Intercomparison of three AATSR Level 2 (L2) AOD products over China, Atmos. Chem. Phys., 16, 9655–9674,

https://doi.org/10.5194/egusphere-2023-1710
Preprint. Discussion started: 13 September 2023

https://doi.org/10.5194/acp-16-9655-2016, 2016.

Che, Y., Xue, Y., Guang, J., She, L., and Guo, J.: Evaluation of the AVHRR DeepBlue aerosol optical depth dataset over mainland China, ISPRS J. Photogramm. Remote Sens., 146, 74–90, https://doi.org/10.1016/j.isprsjprs.2018.09.004, 2018.

Che, Y., Yu, B., Parsons, K., Desha, C., and Ramezani, M.: Evaluation and comparison of MERRA-2 AOD and DAOD with MODIS DeepBlue and AERONET data in Australia, Atmos. Environ., 277, 119054, https://doi.org/10.1016/j.atmosenv.2022.119054, 2022.

Chen, L., Mengersen, K., and Tong, S.: Spatiotemporal relationship between particle air pollution and respiratory emergency hospital admissions in Brisbane, Australia, Sci. Total Environ., 373, 57–67, https://doi.org/10.1016/j.scitotenv.2006.10.050, 2007.

Chen, W., Meng, H., Song, H., and Zheng, H.: Progress in Dust Modelling, Global Dust Budgets, and Soil Organic Carbon Dynamics, Land, 11, 176, https://doi.org/10.3390/land11020176, 2022.

Chepil, W. S. and Woodruff, N. P.: Sedimentary characteristics of dust storms; Part II, Visibility and dust concentration, Am. J. Sci., 255, 104–114, https://doi.org/10.2475/ajs.255.2.104, 1957.

Cowie, G., Lawson, W., and Kim, N.: Australian dust causing respiratory disease admissions in some North Island, New Zealand Hospitals, N. Z. Med. J., 123, 87–88, 2010.

De Deckker, P.: An evaluation of Australia as a major source of dust, Earth-Science Rev., 194, 536–567, https://doi.org/10.1016/j.earscirev.2019.01.008, 2019.

Di, A., Xue, Y., Yang, X., Leys, J., Guang, J., Mei, L., Wang, J., She, L., Hu, Y., He, X., Che, Y., and Fan, C.: Dust aerosol optical depth retrieval and dust storm detection for Xinjiang Region using Indian national satellite observations, Remote Sens., 8, 702, https://doi.org/10.3390/rs8090702, 2016.

Domínguez-Rodríguez, A., Báez-Ferrer, N., Abreu-González, P., Rodríguez, S., Díaz, R., Avanzas, P., and Hernández-Vaquero, D.: Impact of Desert Dust Events on the Cardiovascular Disease: A Systematic Review and Meta-Analysis, J. Clin. Med., 10, 727, https://doi.org/10.3390/jcm10040727, 2021.

Dubovik, O. and King, M. D.: A flexible inversion algorithm for retrieval of aerosol optical properties from Sun and sky radiance measurements, J. Geophys. Res. Atmos., 105, 20673–20696, https://doi.org/10.1029/2000JD900282, 2000.

Ekström, M., McTainsh, G. H., and Chappell, A.: Australian dust storms: temporal trends and relationships with synoptic pressure distributions (1960-99), Int. J. Climatol., 24, 1581–1599, https://doi.org/10.1002/joc.1072, 2004.

https://doi.org/10.5194/egusphere-2023-1710
Preprint. Discussion started: 13 September 2023

741 Fryrear, D. W., Stout, J. E., Hagen, L. J., and Vories, E. D.: Wind erosion: field measurement and analysis, Trans.
742 Am. Soc. Agric. Eng., 34, 155–160, https://doi.org/10.13031/2013.31638, 1991.
743 Gelaro, R., McCarty, W., Suárez, M. J., Todling, R., Molod, A., Takacs, L., Randles, C. A., Darmenov, A.,
744 Bosilovich, M. G., Reichle, R., Wargan, K., Coy, L., Cullather, R., Draper, C., Akella, S., Buchard, V., Conaty,
745 A., da Silva, A. M., Gu, W., Kim, G. K., Koster, R., Lucchesi, R., Merkova, D., Nielsen, J. E., Partyka, G., Pawson,
746 S., Putman, W., Rienecker, M., Schubert, S. D., Sienkiewicz, M., and Zhao, B.: The modern-era retrospective
747 analysis for research and applications, version 2 (MERRA-2), J. Clim., 30, 5419–5454,
748 https://doi.org/10.1175/JCLI-D-16-0758.1, 2017.
749 Giles, D. M., Sinyuk, A., Sorokin, M. G., Schafer, J. S., Smirnov, A., Slutsker, I., Eck, T. F., Holben, B. N., Lewis,
750 J. R., Campbell, J. R., Welton, E. J., Korkin, S. V., and Lyapustin, A. I.: Advancements in the Aerosol Robotic
751 Network (AERONET) Version 3 database - Automated near-real-time quality control algorithm with improved
752 cloud screening for Sun photometer aerosol optical depth (AOD) measurements, Atmos. Meas. Tech., 12, 169–
753 209, https://doi.org/10.5194/amt-12-169-2019, 2019.
754 Ginoux, P., Chin, M., Tegen, I., Prospero, J. M., Holben, B., Dubovik, O., and Lin, S.-J.: Sources and distributions
755 of dust aerosols simulated with the GOCART model, J. Geophys. Res. Atmos., 106, 20255–20273,
756 https://doi.org/10.1029/2000JD000053, 2001.
757 Ginoux, P., Garbuzov, D., and Hsu, N. C.: Identification of anthropogenic and natural dust sources using moderate
758 resolution imaging spectroradiometer (MODIS) deep blue level 2 data, J. Geophys. Res. Atmos., 115, 1–10,
759 https://doi.org/10.1029/2009JD012398, 2010.
760 Ginoux, P., Prospero, J. M., Gill, T. E., Hsu, N. C., and Zhao, M.: Global-scale attribution of anthropogenic and
761 natural dust sources and their emission rates based on MODIS Deep Blue aerosol products, Rev. Geophys., 50,
762 1–36, https://doi.org/10.1029/2012RG000388, 2012.
763 Gkikas, A., Proestakis, E., Amiridis, V., Kazadzis, S., Di Tomaso, E., Tsekeri, A., Marinou, E., Hatzianastassiou,
764 N., and Pérez Garciá-Pando, C.: ModIs Dust AeroSol (MIDAS): A global fine-resolution dust optical depth data
765 set, Atmos. Meas. Tech., 14, 309–334, https://doi.org/10.5194/amt-14-309-2021, 2021.
766 Goudie, A. S.: Desert dust and human health disorders, Environ. Int., 63, 101–113,
767 https://doi.org/10.1016/j.envint.2013.10.011, 2014.
768 Hsu, N. C., Tsay, S. C., King, M. D., and Herman, J. R.: Aerosol properties over bright-reflecting source regions,
769 IEEE Trans. Geosci. Remote Sens., 42, 557–569, https://doi.org/10.1109/TGRS.2004.824067, 2004.

https://doi.org/10.5194/egusphere-2023-1710
Preprint. Discussion started: 13 September 2023

Hsu, N. C., Jeong, M. J., Bettenhausen, C., Sayer, A. M., Hansell, R., Seftor, C. S., Huang, J., and Tsay, S. C.: Enhanced Deep Blue aerosol retrieval algorithm: The second generation, J. Geophys. Res. Atmos., 118, 9296–9315, https://doi.org/10.1002/jgrd.50712, 2013.

Jeffrey, S. J., Carter, J. O., Moodie, K. B., and Beswick, A. R.: Using spatial interpolation to construct a comprehensive archive of Australian climate data, Environ. Model. Softw., 16, 309–330, https://doi.org/10.1016/S1364-8152(01)00008-1, 2001.

de Jesus, A. L., Thompson, H., Knibbs, L. D., Hanigan, I., De Torres, L., Fisher, G., Berko, H., and Morawska, L.: Two decades of trends in urban particulate matter concentrations across Australia, Environ. Res., 190, 110021, https://doi.org/10.1016/j.envres.2020.110021, 2020.

Kolmonen, P., Sogacheva, L., Virtanen, T. H., de Leeuw, G., and Kulmala, M.: The ADV/ASV AATSR aerosol retrieval algorithm: current status and presentation of a full-mission AOD dataset, Int. J. Digit. Earth, 9, 545–561, https://doi.org/10.1080/17538947.2015.1111450, 2016.

de Leeuw, G., Holzer-Popp, T., Bevan, S., Davies, W. H., Descloitres, J., Grainger, R. G., Griesfeller, J., Heckel, A., Kinne, S., Klüser, L., Kolmonen, P., Litvinov, P., Martynenko, D., North, P., Ovigneur, B., Pascal, N., Poulsen, C., Ramon, D., Schulz, M., Siddans, R., Sogacheva, L., Tanré, D., Thomas, G. E., Virtanen, T. H., von Hoyningen Huene, W., Vountas, M., and Pinnock, S.: Evaluation of seven European aerosol optical depth retrieval algorithms for climate analysis, Remote Sens. Environ., 162, 295–315, https://doi.org/10.1016/j.rse.2013.04.023, 2015.

Levy, R. C., Mattoo, S., Munchak, L. A., Remer, L. A., Sayer, A. M., Patadia, F., and Hsu, N. C.: The Collection 6 MODIS aerosol products over land and ocean, Atmos. Meas. Tech., 6, 2989–3034, https://doi.org/10.5194/amt-6-2989-2013, 2013.

Leys, J. F., Heidenreich, S. K., Strong, C. L., McTainsh, G. H., and Quigley, S.: PM10 concentrations and mass transport during " Red Dawn" - Sydney 23 September 2009, Aeolian Res., 3, 327–342, https://doi.org/10.1016/j.aeolia.2011.06.003, 2011.

Love, B. M., Leys, J. F., Strong, C. L., and McTainsh, G. H.: Dust climatology of Mildura, Victoria, Australia: transport direction, Earth Surf. Process. Landforms, 44, 1449–1459, https://doi.org/10.1002/esp.4587, 2019.

Ma, X., Yan, P., Zhao, T., Jia, X., Jiao, J., Ma, Q., Wu, D., Shu, Z., Sun, X., and Habtemicheal, B. A.: Evaluations of surface pm10 concentration and chemical compositions in merra-2 aerosol reanalysis over central and eastern china, Remote Sens., 13, 1317, https://doi.org/10.3390/rs13071317, 2021.

McGowan, H. A. and Clark, A.: A vertical profile of PM10 dust concentrations measured during a regional dust

https://doi.org/10.5194/egusphere-2023-1710
Preprint. Discussion started: 13 September 2023

799 event identified by MODIS Terra, western Queensland, Australia, J. Geophys. Res. Earth Surf., 113, 2–03,
800 https://doi.org/10.1029/2007JF000765, 2008.
801 McGowan, H. A., McTainsh, G. H., Zawar-Reza, P., and Sturman, A. P.: Identifying regional dust transport
802 pathways: Application of kinematic trajectory modelling to a trans-Tasman case, Earth Surf. Process. Landforms,
803 25, 633–647, https://doi.org/10.1002/1096-9837(200006)25:6<633::AID-ESP102>3.0.CO;2-J, 2000.
804 McTainsh, G. H. and Boughton, W. C.: Land Degradation Processes in Australia, Longman Cheshire, Melbourne,
805 389 pp., https://doi.org/10.3/JQUERY-UI.JS, 1993.
806 McTainsh, G. H. and Pitblado, J. R.: Dust storms and related phenomena measured from meteorological records
807 in Australia, Earth Surf. Process. Landforms, 12, 415–424, https://doi.org/10.1002/esp.3290120407, 1987.
808 McTainsh, G. H., Burgess, R., and Pitblado, J. R.: Aridity, drought and dust storms in Australia (1960-84), J. Arid
809 Environ., 16, 11–22, https://doi.org/10.1016/s0140-1963(18)31042-5, 1989a.
810 McTainsh, G. H., Burgess, R., and Pitblado, J. R.: Aridity, drought and dust storms in Australia (1960–84), J.
811 Arid Environ., 16, 11–22, https://doi.org/10.1016/S0140-1963(18)31042-5, 1989b.
812 McTainsh, G. H., Lynch, A. W., and Burgess, R. C.: Wind erosion in eastern australia, Aust. J. Soil Res., 28, 323–
813 339, https://doi.org/10.1071/SR9900323, 1990.
814 McTainsh, G. H., Lynch, A. W., and Tews, E. K.: Climatic controls upon dust storm occurrence in eastern
815 Australia, J. Arid Environ., 39, 457–466, https://doi.org/10.1006/jare.1997.0373, 1998.
816 McTainsh, G. H., Chan, Y. C., McGowan, H., Leys, J., and Tews, K.: The 23rd October 2002 dust storm in eastern
817 Australia: Characteristics and meteorological conditions, Atmos. Environ., 39, 1227–1236,
818 https://doi.org/10.1016/j.atmosenv.2004.10.016, 2005.
819 McTainsh, G. H., Leys, J., O'Loingsigh, T., and Strong, C. L.: Update of Dust Storm Index (DSI) maps for 2005
820 to 2010 and re-analysis and mapping of DSI for for the Australian Collaborative Rangeland Information System
821 (ACRIS), Canberra: DSEWPaC, 1992–2008 pp., 2011a.
822 McTainsh, G. H., Leys, J. F., O'Loingsigh, T., and Strong, C. L.: Wind erosion and land management in Australia
823 during 1940-1949 and 2000-2009, Canberra, 2011b.
824 Mei, L., Xue, Y., de Leeuw, G., von Hoyningen-Huene, W., Kokhanovsky, A. A., Istomina, L., Guang, J., and
825 Burrows, J. P.: Aerosol optical depth retrieval in the Arctic region using MODIS data over snow, Remote Sens.
826 Environ., 128, 234–245, https://doi.org/10.1016/j.rse.2012.10.009, 2013a.
827 Mei, L., Xue, Y., Kokhanovsky, A. A., von Hoyningen-Huene, W., Istomina, L., de Leeuw, G., Burrows, J. P.,

https://doi.org/10.5194/egusphere-2023-1710
Preprint. Discussion started: 13 September 2023

828 Guang, J., and Jing, Y.: Aerosol optical depth retrieval over snow using AATSR data, Int. J. Remote Sens., 34,
829 5030–5041, https://doi.org/10.1080/01431161.2013.786197, 2013b.
830 Middleton, N. J.: Desert dust hazards: A global review, Aeolian Res., 24, 53–63,
831 https://doi.org/10.1016/j.aeolia.2016.12.001, 2017.
832 Mukkavilli, S. K., Prasad, A. A., Taylor, R. A., Huang, J., Mitchell, R. M., Troccoli, A., and Kay, M. J.:
833 Assessment of atmospheric aerosols from two reanalysis products over Australia, Atmos. Res., 215, 149–164,
834 https://doi.org/10.1016/j.atmosres.2018.08.026, 2019.
835 O'Loingsigh, T., McTainsh, G. H., Tapper, N. J., and Shinkfield, P.: Lost in code: A critical analysis of using
836 meteorological data for wind erosion monitoring, Aeolian Res., 2, 49–57,
837 https://doi.org/10.1016/j.aeolia.2010.03.002, 2010.
838 O'Loingsigh, T., McTainsh, G. H., Tews, E. K., Strong, C. L., Leys, J. F., Shinkfield, P., and Tapper, N. J.: The
839 Dust Storm Index (DSI): A method for monitoring broadscale wind erosion using meteorological records, Aeolian
840 Res., 12, 29–40, https://doi.org/10.1016/j.aeolia.2013.10.004, 2014.
841 O'Loingsigh, T., Chubb, T., Baddock, M., Kelly, T., Tapper, N. J., de Deckker, P., and McTainsh, G.: Sources
842 and pathways of dust during the Australian "millennium drought" decade, J. Geophys. Res., 122, 1246–1260,
843 https://doi.org/10.1002/2016JD025737, 2017.
844 Ou, Y., Li, Z., Chen, C., Zhang, Y., Li, K., Shi, Z., Dong, J., Xu, H., Peng, Z., Xie, Y., and Luo, J.: Evaluation of
845 MERRA-2 Aerosol Optical and Component Properties over China Using SONET and PARASOL/GRASP Data,
846 Remote Sens., 14, https://doi.org/10.3390/rs14040821, 2022.
847 Pereira, G., Lee, H. J., Bell, M., Regan, A., Malacova, E., Mullins, B., and Knibbs, L. D.: Development of a model
848 for particulate matter pollution in Australia with implications for other satellite-based models, Environ. Res., 159,
849 9–15, https://doi.org/10.1016/j.envres.2017.07.044, 2017.
850 Prospero, J. M., Barkley, A. E., Gaston, C. J., Gatineau, A., Campos y Sansano, A., and Panechou, K.:
851 Characterizing and Quantifying African Dust Transport and Deposition to South America: Implications for the
852 Phosphorus Budget in the Amazon Basin, Global Biogeochem. Cycles, 34, e2020GB006536,
853 https://doi.org/10.1029/2020GB006536, 2020.
854 Provençal, S., Buchard, V., da Silva, A. M., Leduc, R., and Barrette, N.: Evaluation of PM surface concentrations
855 simulated by Version 1 of NASA's MERRA Aerosol Reanalysis over Europe, Atmos. Pollut. Res., 8, 374–382,
856 https://doi.org/10.1016/j.apr.2016.10.009, 2017.

https://doi.org/10.5194/egusphere-2023-1710
Preprint. Discussion started: 13 September 2023

Pu, B. and Ginoux, P.: Projection of American dustiness in the late 21st century due to climate change, Sci. Rep., 7, https://doi.org/10.1038/s41598-017-05431-9, 2017.

Pu, B. and Ginoux, P.: How reliable are CMIP5 models in simulating dust optical depth?, Atmos. Chem. Phys., 18, 12491–12510, https://doi.org/10.5194/acp-18-12491-2018, 2018.

Qin, W., Zhang, Y., Chen, J., Yu, Q., Cheng, S., Li, W., Liu, X., and Tian, H.: Variation, sources and historical trend of black carbon in Beijing, China based on ground observation and MERRA-2 reanalysis data, Environ. Pollut., 245, 853–863, https://doi.org/10.1016/j.envpol.2018.11.063, 2019.

Randles, C. A., da Silva, A. M., Buchard, V., Colarco, P. R., Darmenov, A., Govindaraju, R., Smirnov, A., Holben, B., Ferrare, R., Hair, J., Shinozuka, Y., and Flynn, C. J.: The MERRA-2 aerosol reanalysis, 1980 onward. Part I: System description and data assimilation evaluation, J. Clim., 30, 6823–6850, https://doi.org/10.1175/JCLI-D-16-0609.1, 2017.

Roberts, S.: Have the short-term mortality effects of particulate matter air pollution changed in Australia over the period 1993-2007?, Environ. Pollut., 182, 9–14, https://doi.org/10.1016/j.envpol.2013.06.036, 2013.

Rotstayn, L. D., Collier, M. A., Mitchell, R. M., Qin, Y., Campbell, S. K., and Dravitzki, S. M.: Simulated enhancement of ENSO-related rainfall variability due to Australian dust, Atmos. Chem. Phys., 11, 6575–6592, https://doi.org/10.5194/ACP-11-6575-2011, 2011.

RUST, B. R. and NANSON, G. C.: Bedload transport of mud as pedogenic aggregates in modern and ancient rivers, Sedimentology, 36, 291–306, https://doi.org/10.1111/j.1365-3091.1989.tb00608.x, 1989.

Sayer, A. M., Hsu, N. C., Bettenhausen, C., and Jeong, M. J.: Validation and uncertainty estimates for MODIS Collection 6 “deep Blue” aerosol data, J. Geophys. Res. Atmos., 118, 7864–7872, https://doi.org/10.1002/jgrd.50600, 2013.

Sayer, A. M., Hsu, N. C., Lee, J., Carletta, N., Chen, S. H., and Smirnov, A.: Evaluation of NASA Deep Blue/SOAR aerosol retrieval algorithms applied to AVHRR measurements, J. Geophys. Res. Atmos., 122, 9945–9967, https://doi.org/10.1002/2017JD026934, 2017.

Sayer, A. M., Hsu, N. C., Lee, J., Kim, W. V., and Dutcher, S. T.: Validation, Stability, and Consistency of MODIS Collection 6.1 and VIIRS Version 1 Deep Blue Aerosol Data Over Land, J. Geophys. Res. Atmos., 124, 4658–4688, https://doi.org/10.1029/2018JD029598, 2019.

Shao, Y.: Physics and Modelling of Wind Erosion, Phys. Model. Wind Eros., 452, https://doi.org/10.1007/978-1-4020-8895-7, 2009.

https://doi.org/10.5194/egusphere-2023-1710
Preprint. Discussion started: 13 September 2023

886 Shao, Y., Yang, Y., Wang, J., Song, Z., Leslie, L. M., Dong, C., Zhang, Z., Lin, Z., Kanai, Y., Yabuki, S., and
887 Chun, Y.: Northeast Asian dust storms: Real-time numerical prediction and validation, J. Geophys. Res. Atmos.,
888 108, 2003JD003667, https://doi.org/10.1029/2003JD003667, 2003.
889 Shao, Y., Leys, J. F., McTainsh, G. H., and Tews, K.: Numerical simulation of the October 2002 dust event in
890 Australia, J. Geophys. Res. Atmos., 112, 8207, https://doi.org/10.1029/2006JD007767, 2007.
891 Shao, Y., Klose, M., and Wyrwoll, K.-H.: Recent global dust trend and connections to climate forcing, J. Geophys.
892 Res. Atmos., 118, 11,107-11,118, https://doi.org/10.1002/jgrd.50836, 2013.
893 Shaylor, M., Brindley, H., and Sellar, A.: An Evaluation of Two Decades of Aerosol Optical Depth Retrievals
894 from MODIS over Australia, Remote Sens., 14, 2664, https://doi.org/10.3390/rs14112664, 2022.
895 She, L., Xue, Y., Guang, J., Che, Y., Fan, C., Li, Y., and Xie, Y.: Towards a comprehensive view of dust events
896 from multiple satellite and ground measurements: Exemplified by the May 2017 East Asian dust storm, Nat.
897 Hazards Earth Syst. Sci., 18, 3187–3201, https://doi.org/10.5194/nhess-18-3187-2018, 2018.
898 Song, Q., Zhang, Z., Yu, H., Ginoux, P., and Shen, J.: Global dust optical depth climatology derived from CALIOP
899 and MODIS aerosol retrievals on decadal timescales: regional and interannual variability, Atmos. Chem. Phys.,
900 21, 13369–13395, https://doi.org/10.5194/acp-21-13369-2021, 2021.
901 Soni, A., Mandariya, A. K., Rajeev, P., Izhar, S., Singh, G. K., Choudhary, V., Qadri, A. M., Gupta, A. D., Singh,
902 A. K., and Gupta, T.: Multiple site ground-based evaluation of carbonaceous aerosol mass concentrations retrieved
903 from CAMS and MERRA-2 over the Indo-Gangetic Plain, Environ. Sci. Atmos., 1, 577–590,
904 https://doi.org/10.1039/d1ea00067e, 2021.
905 Speer, M. S.: Dust storm frequency and impact over Eastern Australia determined by state of Pacific climate
906 system, Weather Clim. Extrem., 2, 16–21, https://doi.org/10.1016/j.wace.2013.10.004, 2013.
907 Sprigg, R. C.: Alternating wind cycles of the Quaternary era and their influences on aeolian sedimentation in and
908 around the dune deserts of south-eastern Australia, in: Quaternary Dust Mantles of China, New Zealand and
909 Australia, 1982.
910 Stefanski, R. and Sivakumar, M. V. K.: Impacts of sand and dust storms on agriculture and potential agricultural
911 applications of a SDSWS, IOP Conf. Ser. Earth Environ. Sci., 7, 012016, https://doi.org/10.1088/1755-
912 1307/7/1/012016, 2009.
913 Strong, C. L., Parsons, K., McTainsh, G. H., and Sheehan, A.: Dust transporting wind systems in the lower Lake
914 Eyre Basin, Australia: A preliminary study, Aeolian Res., 2, 205–214,

https://doi.org/10.5194/egusphere-2023-1710
Preprint. Discussion started: 13 September 2023

915 https://doi.org/10.1016/j.aeolia.2010.11.001, 2011.
916 Sun, E., Xu, X., Che, H., Tang, Z., Gui, K., An, L., Lu, C., and Shi, G.: Variation in MERRA-2 aerosol optical
917 depth and absorption aerosol optical depth over China from 1980 to 2017, J. Atmos. Solar-Terrestrial Phys., 186,
918 8–19, https://doi.org/10.1016/j.jastp.2019.01.019, 2019a.
919 Sun, E., Che, H., Xu, X., Wang, Z., Lu, C., Gui, K., Zhao, H., Zheng, Y., Wang, Y., Wang, H., Sun, T., Liang, Y.,
920 Li, X., Sheng, Z., An, L., Zhang, X., and Shi, G.: Variation in MERRA-2 aerosol optical depth over the Yangtze
921 River Delta from 1980 to 2016, Theor. Appl. Climatol., 136, 363–375, https://doi.org/10.1007/s00704-018-2490-
922 9, 2019b.
923 Sundström, A. M., Kolmonen, P., Sogacheva, L., and de Leeuw, G.: Aerosol retrievals over China with the
924 AATSR dual view algorithm, Remote Sens. Environ., 116, 189–198, https://doi.org/10.1016/j.rse.2011.04.041,
925 2012.
926 Tanaka, T. Y. and Chiba, M.: A numerical study of the contributions of dust source regions to the global dust
927 budget, Glob. Planet. Change, 52, 88–104, https://doi.org/10.1016/j.gloplacha.2006.02.002, 2006.
928 Tews, K.: Wind erosion rates from meteorological records in eastern Australia 1960-92, Griffith University, 1996.
929 Thomas, G. E., Carboni, E., Sayer, A. M., Poulsen, C. A., Siddans, R., and Grainger, R. G.: Oxford-RAL Aerosol
930 and Cloud (ORAC): aerosol retrievals from satellite radiometers, Satell. Aerosol Remote Sens. over L., 193–225,
931 https://doi.org/10.1007/978-3-540-69397-0_7, 2009.
932 Torre, G., Gaiero, D., Coppo, R., Cosentino, N. J., Goldstein, S. L., De Vleeschouwer, F., Roux, G. Le, Bolge, L.,
933 Kiro, Y., and Sawakuchi, A. O.: Unraveling late Quaternary atmospheric circulation in the Southern Hemisphere
934 through the provenance of Pampean loess, Earth-Science Rev., 232, 104143,
935 https://doi.org/10.1016/j.earscirev.2022.104143, 2022.
936 Tozer, P. and Leys, J.: Dust storms - What do they really cost?, Rangel. J., 35, 131–142,
937 https://doi.org/10.1071/RJ12085, 2013.
938 Voss, K. K. and Evan, A. T.: A new satellite-based global climatology of dust aerosol optical depth, J. Appl.
939 Meteorol. Climatol., 59, 83–102, https://doi.org/10.1175/JAMC-D-19-0194.1, 2020.
940 Wei, J., Li, Z., Peng, Y., and Sun, L.: MODIS Collection 6.1 aerosol optical depth products over land and ocean:
941 validation and comparison, Atmos. Environ., 201, 428–440, https://doi.org/10.1016/j.atmosenv.2018.12.004,
942 2019.
943 Wu, C., Lin, Z., and Liu, X.: The global dust cycle and uncertainty in CMIP5 (Coupled Model Intercomparison

https://doi.org/10.5194/egusphere-2023-1710
Preprint. Discussion started: 13 September 2023

944 Project phase 5) models, Atmos. Chem. Phys., 20, 10401–10425, https://doi.org/10.5194/acp-20-10401-2020,
945 2020.
946 Yang, L., She, L., Che, Y., He, X., Yang, C., and Feng, Z.: Analysis of Dust Detection Algorithms Based on FY-
947 4A Satellite Data, Appl. Sci., 13, 1365, https://doi.org/10.3390/app13031365, 2023.
948 Yang, X., Zhao, C., Yang, Y., and Fan, H.: Long-term multi-source data analysis about the characteristics of
949 aerosol optical properties and types over Australia, Atmos. Chem. Phys., 21, 3803–3825,
950 https://doi.org/10.5194/acp-21-3803-2021, 2021.
951 Yu, B., Neil, D. T., and Hesse, P. P.: Correlation between rainfall and dust occurrence at mildura, Australia: The
952 difference between local and source area rainfalls, Earth Surf. Process. Landforms, 17, 723–727,
953 https://doi.org/10.1002/esp.3290170708, 1992.
954 Yu, B., Hesse, P. P., and Neil, D. T.: The relationship between antecedent regional rainfall conditions and the
955 occurrence of dust events at Mildura, Australia, J. Arid Environ., 24, 109–124,
956 https://doi.org/10.1006/jare.1993.1010, 1993.
957 Yu, Y. and Ginoux, P.: Assessing the contribution of the ENSO and MJO to Australian dust activity based on
958 satellite- And ground-based observations, Atmos. Chem. Phys., 21, 8511–8530, https://doi.org/10.5194/acp-21-
959 8511-2021, 2021.
960 Zender, C. S.: Mineral Dust Entrainment and Deposition (DEAD) model: Description and 1990s dust climatology,
961 J. Geophys. Res., 108, 4416, https://doi.org/10.1029/2002JD002775, 2003.
962 Zhang, X., Zhao, L., Tong, D. Q., Wu, G., Dan, M., and Teng, B.: A systematic review of global desert dust and
963 associated human health effects, Atmosphere (Basel)., 7, https://doi.org/10.3390/atmos7120158, 2016.
964 Zhao, Q., Zhao, W., Bi, J., and Ma, Z.: Climatology and calibration of MERRA-2 PM2.5 components over China,
965 Atmos. Pollut. Res., 12, 357–366, https://doi.org/10.1016/j.apr.2020.11.016, 2021.
966